④

# David Taylor Research Center

Bethesda, MD 20084-5000

# Electrical Characteristics of a Seawater MHD Thruster

by
Kenneth E. Tempelmeyer
Visiting Secretary of the Navy Fellow at U.S. Naval Academy
and
David Taylor Research Center Consultant

90 07 25 092

# MAJOR DTRC TECHNICAL COMPONENTS

CODE 011  DIRECTOR OF TECHNOLOGY, PLANS AND ASSESSMENT

12  SHIP SYSTEMS INTEGRATION DEPARTMENT

14  SHIP ELECTROMAGNETIC SIGNATURES DEPARTMENT

15  SHIP HYDROMECHANICS DEPARTMENT

16  AVIATION DEPARTMENT

17  SHIP STRUCTURES AND PROTECTION DEPARTMENT

18  COMPUTATION, MATHEMATICS & LOGISTICS DEPARTMENT

19  SHIP ACOUSTICS DEPARTMENT

27  PROPULSION AND AUXILIARY SYSTEMS DEPARTMENT

28  SHIP MATERIALS ENGINEERING DEPARTMENT

---

## DTRC ISSUES THREE TYPES OF REPORTS:

1. **DTRC reports, a formal series,** contain information of permanent technical value. They carry a consecutive numerical identification regardless of their classification or the originating department.

2. **Departmental reports, a semiformal series,** contain information of a preliminary, temporary, or proprietary nature or of limited interest or significance. They carry a departmental alphanumerical identification.

3. **Technical memoranda, an informal series,** contain technical documentation of limited use and interest. They are primarily working papers intended for internal use. They carry an identifying number which indicates their type and the numerical code of the originating department. Any distribution outside DTRC must be approved by the head of the originating department on a case-by-case basis.

# REPORT DOCUMENTATION PAGE

| 1a. REPORT SECURITY CLASSIFICATION<br>Unclassified | | 1b. RESTRICTIVE MARKINGS | | | |
| --- | --- | --- | --- | --- | --- |
| 2a. SECURITY CLASSIFICATION AUTHORITY | | 3. DISTRIBUTION AVAILABILITY OF REPORT | | | |
| 2b. DECLASSIFICATION DOWNGRADING SCHEDULE | | Approved for public release; distribution is unlimited. | | | |
| 4. PERFORMING ORGANIZATION REPORT NUMBER(S)<br><br>DTRC-90/017 | | 5. MONITORING ORGANIZATION REPORT NUMBER(S) | | | |
| 6a. NAME OF PERFORMING ORGANIZATION<br><br>David Taylor Research Center | 6b. OFFICE SYMBOL<br>(If applicable)<br><br>Code 2712 | 7a. NAME OF MONITORING ORGANIZATION | | | |
| 6c. ADDRESS (City, State and ZIP Code)<br><br>Bethesda, MD 20084-5000 | | 7b. ADDRESS (City, State and ZIP Code) | | | |
| 8a. NAME OF FUNDING SPONSORING<br>ORGANIZATION | 8b. OFFICE SYMBOL<br>(If applicable)<br><br>DTC C0113 | 9. PROCUREMENT INSTRUMENT IDENTIFICATION NUMBER | | | |
| 8c. ADDRESS (City, State and ZIP Code)<br><br>DTRC<br>Bethesda, Maryland 20084-5000 | | 10. SOURCE OF FUNDING NUMBERS | | | |
| | | PROGRAM ELEMENT NO<br><br>62936N | PROJECT NO<br><br>1-2712-131 | TASK NO<br><br>ZF66412000 | WORK UNIT ACCESSION NO<br><br>500540 |

| 11. TITLE (Include Security Classification)<br><br>Electrical Characteristics of a Seawater MHD Thruster | | | |
| --- | --- | --- | --- |
| 12. PERSONAL AUTHOR(S)<br><br>Kenneth E. Tempelmeyer | | | |
| 13a. TYPE OF REPORT<br><br>Final | 13b. TIME COVERED<br>FROM_____ TO_____ | 14. DATE OF REPORT (YEAR, MONTH, DAY)<br><br>June 1990 | 15. PAGE COUNT<br><br>39 |

| 16. SUPPLEMENTARY NOTATION<br><br>This work was a cooperative effort with the United States Naval Academy, Annapolis, Maryland 21402. |
| --- |

| 17. | COSATI CODES | | 18. SUBJECT TERMS (Continue on reverse if necessary and identify by block number) |
| --- | --- | --- | --- |
| FIELD | GROUP | SUB-GROUP | Seawater |
| | | | Magnetohydrodynamic thruster electrical conductivity |

19. ABSTRACT (Continue on reverse if necessary and identify by block number)

There is renewed interest in the application of the magnetohydrodynamic (MHD) propulsion concept to marine propulsion. However, there is almost no experimental information concerning the major physical processes which will occur in a seawater MHD propulsion unit, such as (1) the seawater electrolysis process at operational conditions needed for ship propulsion, (2) the effects of bubble formation on the performance of a seawater thruster and (3) the effectiveness of the MHD interaction in seawater. Small scale tests of an MHD type channel but without an applied magnetic field have been carried out to provide information about the first two of these areas (1) seawater electrolysis and (2) the effect of the $H_2$ bubbles generated during the electrolysis of seawater. Current/voltage characteristics were obtained with different electrode materials for current densities up to 0.3 amp/$cm^2$. The effect of bubble formation on the channel current has been assessed over a range of operating conditions. Long-duration tests to 100 hrs have been made to provide information on electrode durability and long-term operational problems.

| 20. DISTRIBUTION/AVAILABILITY OF ABSTRACT<br><br>☒ UNCLASSIFIED/UNLIMITED ☐ SAME AS RPT ☐ DTIC USERS | 21. ABSTRACT SECURITY CLASSIFICATION<br><br>Unclassified | |
| --- | --- | --- |
| 22a. NAME OF RESPONSIBLE INDIVIDUAL<br><br>Samuel H. Brown | 22b. TELEPHONE (Include Area Code)<br><br>(301)-267-2146 | 22c. OFFICE SYMBOL<br><br>Code 2712 |

**DD FORM 1473**, JUN 86      *Previous editions are obsolete.*

# CONTENTS

## FIGURES

## TABLES

Accession For

NTIS  CRA&I

DTIC TAB

Unannounced

Justification

By

Distribution/

Availability Codes

Avail and/or

Dist   Special

A-1

## ABSTRACT

*There is renewed interest in the application of the magnetohydrodynamic (MHD) propulsion concept to marine propulsion. However, there is almost no experimental information concerning the major physical processes which will occur in a seawater MHD propulsion unit, such as (1) the seawater electrolysis process at operational conditions needed for ship propulsion, (2) the effects of bubble formation on the performance of a seawater thruster and (3) the effectiveness of the MHD interaction in seawater. Small scale tests of an MHD type channel but without an applied magnetic field have been carried out to provide information about the first two of these areas (1) seawater electrolysis and (2) the effect of the $H_2$ bubbles generated during the electrolysis of seawater. Current/voltage characteristics were obtained with different electrode materials for current densities up to 0.3 amp/cm$^2$. The effect of bubble formation on the channel current has been assessed over a range of operating conditions. Long-duration tests to 100 hrs have been made to provide information on electrode durability and long-term operational problems.*

## ADMINISTRATIVE INFORMATION

## INTRODUCTION

The acceleration of electrically conducting fluids by crossed electric and magnetic fields (i.e., electromagnetic pumps) has been proposed and investigated for many years. Commercially available liquid-metal pumps successfully utilize this concept but it has had limited success in other applications.

Because seawater is an electrical conductor, the application of this concept for ship propulsion (i.e. magnetohydrodynamic (MHD) propulsion) has been repeatedly suggested over the past three decades.[1-5] In 1968, Way[6] constructed and operated a model of an MHD powered vessel which was probably the first demonstration of MHD propulsion for ships. More recently there have been several publications as well as news media accounts of MHD ship propulsion research in Japan. This activity is centered at and funded by the Japan Foundation for Shipbuilding Advancement (JAFSA). (See, for example, publications by Tada, et al.[7] and Motora[8].) The Japanese effort is aimed at the operation of a successful prototype which is reported to have two MHD thrusters each producing a Lorentz force of 8000 newtons with a 4 tesla superconducting magnet installed in a vessel having a displacement of about 150 tons.[9]

With the advent of superconducting magnets, which can produce fields of 6 to 10 tesla, the application of MHD thrusters for seawater becomes more feasible. As a result, there is an increasing interest in this propulsion concept at several naval laboratories and at the Defense Advanced Research Project Agency (DARPA). The interest in this ship propulsion concept is stimulated by the potentially quieter operation of an MHD thruster

as compared to a conventional methods of providing mechanical power to shafts and propellers.

The David Taylor Research Center (DTRC) has been analytically studying the application of MHD thrusters for ship propulsion. To support this activity, an experimental test program of the electrical characteristics of an MHD thruster has been started at the U.S. Naval Academy in cooperation with DTRC using two conventional water tables in the Mechanical Engineering Fluids Mechanics Laboratory. The purposes of these tests were to: (1) determine the current-voltage characteristics of an MHD channel flowing with seawater (without an applied magnetic field); (2) determine the electrical conductivity of simulated seawater and the electrode voltage drops; (3) investigate different types of electrode materials; (4) observe the dynamics of bubble formation, hydrogen on the cathode, and chlorine on the anode at various operating conditions, and (5) make measurements of bubble noise downstream of the channel.

This report summarizes the electrical characteristics of a small-scale seawater MHD thruster configuration, but without the applied magnetic field, and provides some comments on the suitability of some different electrode materials. A second DTRC technical report in preparation provides information concerning bubble formation, bubble dynamics and the noise potential of a seawater MHD propulsion unit.

## BACKGROUND

Ohms Law for an MHD thruster may be written as:

$$\vec{j} = \sigma \ (\vec{E}_{app} + \vec{V} \times \vec{B})$$ (1)

where $\vec{E}app$ represents the applied electric field provided by an external d-c power supply and $\vec{V} \times \vec{B}$ is the electric field induced by the motion of the conductor through the magnetic field. There was no applied magnetic field for the tests described here $\vec{B} = 0$. As a result, the measured current-voltage characteristics for a constant-area rectangular channel are related by:

$$\frac{I}{(L)(W)} = \sigma \frac{V_{app}}{d}$$ (2)

where $L$ and $W$ are the length and width of the electrodes in contact with the salt water and $d$ is the electrode spacing. The experimental current-voltage characteristics presented here (in terms of the current density in j, and the electric field $E$) are representative of what will occur in a seawater MHD thruster when $E$ is interpreted as the sum of the applied and induced electric fields in an MHD unit.

As a voltage is applied across the electrodes, current begins to flow resulting in electrolysis of the salt water. While there has been no attempt in this investigation to study the electrochemical reactions in the electrolysis process, some background may aid in understanding the performance of various electrode materials and other phenomena that occur.

If the electrodes are inert, electrolysis of an aqueous solution NaCl results in the generation of chlorine gas at the anode (positive electrode) and hydrogen gas at the cathode by the reactions:

$$Anode \qquad 2Cl^- \rightarrow Cl_2 + 2e^- \qquad\qquad (3)$$

$$Cathode \qquad 2e^- + 2H_2O \rightarrow H_2 + 2(OH)^- \qquad\qquad (4)$$
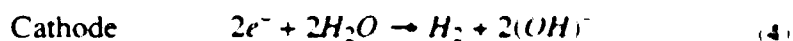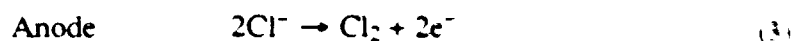
A surplus of electrons at the cathode creates conditions for chemical reduction in that region and the deficit of electrons at the anode results in the conditions for oxidation. However, if the anode material is oxidized, there will be material loss through reactions such as:

$$Al \rightarrow Al^{+++} + 3e \qquad\qquad (5)$$

$$Cu \rightarrow Cu^{++} + 2e \qquad\qquad (6)$$

$$Fe \rightarrow Fe^{++} + 2e \qquad\qquad (7)$$
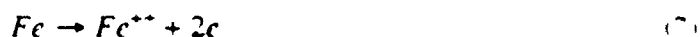
resulting in the formation of oxides of the anode material as the reacting anode material contributes metal ions to the solution. Thus, the principle results of passing an electric current through seawater are the production of $H_2$ at the cathode and the oxidation of reacting metals at the anode.

More complicated electrode reactions can also occur depending upon the electrode materials used and the level of current. Bennett[10] states that chlorine generated at the anode will very quickly be hydrolyzed and $H_2$ generated by the reactions

$$2Cl^- \rightarrow Cl_2 + 2e^- \qquad\qquad (8)$$

$$Cl_2 + H_2O \Leftrightarrow HClO + Cl^- + H^+ \qquad\qquad (9)$$

$$HClO \Leftrightarrow H^+ + (ClO)^- \qquad\qquad (10)$$

$$2H^+ + 2e \rightarrow H_2 \qquad\qquad (11)$$
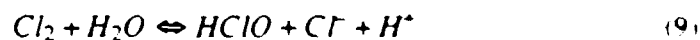
The hypochlorite ion, $(ClO)^-$ produced in this process increases the pH of the solution.

The acid HClO is termed hypochlorous acid. At certain voltage levels $O_2$ generation at the anode may be favored over the production of chlorine through the reaction.

$$2H_2O \rightarrow O_2 + 4H^+ + 4e^- \qquad\qquad (12)$$
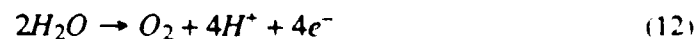
This apparently occurs at very low current densities ($j < 1$ mA/cm$^2$) and is probably not important for the conditions of these tests.

The amount of hydrogen gas produced at the cathode is simple to calculate since one hydrogen atom is produced for every electron. The measurement of the electrolysis current was employed as an early means of determining Avogadro's Number. One Faraday of charge, F, (96,487 coulombs) will produce one mole or 1.008 gms of hydrogen. Thus, a current of 10 amps will result in $1.044 \times 10^{-3}$ gm of H sec. As a result, it can be shown that the volumetric production of H$_2$ is

$$ V = \left(\frac{I}{F}\right) \times \left(\frac{RT}{2P}\right) \tag{13} $$

if H$_2$ is treated as a perfect gas. For typical run conditions of these tests, $T = 300$ K, $p = 1$ atm and at a current of $I = 10$ amp,

$$ V = 1.28 \times 10^{-3} \text{ liters of H}_2/\text{sec} \tag{14} $$

were produced. This represents the maximum H$_2$ gas generation rate for these tests.

Additional chemical reactions also occur in the high pH region near the cathode. Magnesium and calcium salts which are present in seawater are hydrolyzed to form calcium and/or magnesium hydroxide. These oxides exist as a white gelatinous or colloidal material, and the reactions are more predominate with certain types of electrodes where the gelatinous products begin to adhere to surfaces in regions of low velocity. Ca(OH)$_2$ and Mg(OH)$_2$ form routinely in seawater electrolysis cells and are periodically removed by reversing the current.* The formation of these materials, however, may cause additional problems in seawater MHD thrusters.

Additional information concerning seawater electrolysis is available in other references.[11-14]

## TEST EQUIPMENT

### WATER TABLE FACILITY

Tests were carried out using two water tables which produce a sheet of water having a specified depth. Wall guides were introduced to simulate a two-dimensional flow channel consisting of an intake nozzle, a constant area MHD channel (without B-field), and an exit diffuser, see Fig. 1. The channel dimensions were adjustable to accommodate investigation of different channel configurations and sizes. Two basic channel configurations were used:

1. Open-Top Channel - In this configuration the electrodes made up the sidewalls of the channel as shown in Fig. 1. The bottom wall or floor was made of an insulating material and there was a free, water surface at the top. Figure 2a is a photograph of this configuration.

* Niksa, M., Eltech Corp., private communication (June 1989).

2. Closed Channel - When this configuration was used, the bottom surface of the channel served as the cathode; the top surface as the anode; the sidewalls were made from non-conducting materials. This channel was fully submerged in the water flow. A photograph of the closed channel may be seen in Fig 2b.

ELECTRODE MATERIALS

Several electrode materials were investigated as summarized in Table 1 below:

The width or height of the electrodes ($W$) varied from about 2 to 5 cm and the channel and electrode length ($L$) varied from about 12 to 20.5 cm. The electrode spacing ($d$) was also varied but for most tests the spacing between electrodes was about 5 cm.

Long-duration (50 hr or 100 hr) tests were made for electrode pairs 4 and 5.

**Table 1.** Electrode materials tested.

| Pair Number | Channel | |
| | Anode | Cathode |
| --- | --- | --- |
| | *Open-Top Channel* | |
| 1 | Aluminum | Aluminum |
| 2 | Copper | Copper |
| 3 | Incoloy 800 | Incoloy 800 |
| 4 | Mixed-Metal Oxide Coating on a Metallic Substrate* | Mixed-Metal Oxide Coating on a Metallic Substrate* |
| 5 | Mixed-Metal Oxide Coating on a Metallic Substrate* | Hastelloy C |
| | *Closed Channel* | |
| 6 | Aluminum | Aluminum |
| 7 | Copper | Copper |

*DSA® material manufactured and provided by Eltech Corp is "based on inventions using mixed metal oxide coatings usually valve metal and platinum group metal oxides applied to a valve metal (e.g. titanium or tantalum) substrate."

POWER SUPPLY AND INSTRUMENTATION

The electrodes were connected to a D.C. power supply. Applied voltages ranged from 0 to 30 volts; the corresponding current varied from 0 to about 12 amps. The electrode surface area could be varied by changing the depth of the water in the open channel and/or changing the length of the electrodes in the closed channels. Current/voltage measurements were made for each of the electrode pairs by applying various voltages up to the value which produced a current density of 0.2 to 0.3 amp/cm². Approximate calculation of the electrical characteristics of an MHD seawater thruster suggest that this level would be the upper limit of current density which would be of interest.

Currents and voltages were measured with Fluke meters. The repeatability of the electrical measurements was well within 2%.

Approximate values of the flow velocity were obtained from: (1) a water flow meter in the water table and (2) by timing the passage of a small floating object in the MHD

channel. Test velocities varied from 0 up to about 90 cm/sec. The accuracy of the flow velocity measurement was no better than about ±10% of the values stated. Throughout these tests, however, there was no indication that the flow velocity had an important effect upon the measured current and voltage characteristics other than a small effect on the "starting voltage" which is discussed later.

Specific gravity of the simulated seawater was measured periodically with a calibrated hydrometer set and the pH of the water was regularly monitored with a pH cell and meter.

## EXPERIMENTAL RESULTS AND DISCUSSION

### SIMULATION OF SEAWATER

*Electrical Conductivity*

The water tables were drained and filled with fresh tap water having a specific gravity of 1.000. Various potentials were applied across the electrodes with the fresh water flowing through the channel at a velocity of about 20 cm/sec. The current varied linearly with voltage. From the applied voltages and current measurements the fresh water was found to have an electrical conductivity of $\sigma \approx 0.0306$ S/meter.

Salts (in the form of the commercial product named "Instant Ocean") were then added to the water in several steps. At each step the (1) specific gravity and (2) currents at various voltages were measured. As will be observed in subsequent figures, the current varied linearly with voltage for the salt water over the current range provided by the power supply. Figure 3 summarizes the measured electrical conductivity of the simulated seawater as a function of its specific gravity. At a specific gravity of 1.024, a typical value for seawater, the electrical conductivity was found to be 4.5 S/m which is also consistent with typical published values for seawater. Moreover, the electrical conductivity of the simulated seawater varied linearly with the specific gravity of the water up to specific gravities corresponding to ocean water.

For experimental purposes it may be desirable to increase the electrical conductivity of the water well beyond that of seawater. One test was performed on a solution containing twice the amount of Instant Ocean needed to achieve an electrical conductivity of 4.5 S/m. All of the salts were soluable and the resulting conductivity was slightly above 10 S/m with a specific gravity of 1.05. This data point is also shown in Fig. 3. While no attempts were made to produce higher conductivities, it is possible to do so by the addition of larger amounts of an appropriate salt compound. The specific gravity and electrical conductivity of the test medium were maintained near 1.024 and 4.5 S/m respectively throughout the tests reported here.

*Scaling Compounds*

As will be discussed later, longer duration testing of the electrodes resulted in the formation of a gelatinous material on the cathode side of the channel. This material which was principally $Ca(OH)_2$ adhered to some of the cathode materials and to wall surface discontinuities and corners. Whether or not this material will be formed in an MHD thruster operating on seawater is not known. However, these tests indicate that it will

6

form in facilities simulating seawater with Instant Ocean. It can provide some obstruc-
tion to the flow and reduce somewhat the effective surface area. These effects are
discussed later

## CURRENT/VOLTAGE CHARACTERISTICS

The current-voltage characteristics of several types of electrodes were obtained for
the channel geometries and test conditions summarized below

| | |
|---|---|
| (a) Channel Length, $L$ | 12.7 to 20.5 cm |
| (b) Channel Width (Electrode Spacing), $d$ | 5 to 10 cm |
| (c) Electrode Width, $W$ | 2 to 5 cm |
| (d) Flow Velocity, $V$ | 0 to 90 cm/sec |
| (e) Electrical Conductivity, $\sigma$ | 4.1 to 4.5 S/m |

Data given in Figs. 4 through 9 are in terms of applied electric field $E$ and current
density $j$ in order to generalize the variation of channel geometry. Data were obtained
for current densities up to 0.2 to 0.3 amp/cm$^2$ which will probably be the upper level of
current density of interest in seawater MHD thrusters for ship propulsion

### Open Top Channel Configuration

The electrical characteristics of five open-top channels with different electrode ma-
terials are given in Figs. 4 through 8. In all of these tests the electrodes served as the
vertical sidewalls.

It was anticipated that the H$_2$ generation at the cathode might create a gas sheath
over the electrode and produce a non-linear variation of current density with increasing
electric field. Inspection of the Fig. 4 to Fig. 8 data however, illustrates that this does not
occur. Small H$_2$ bubbles formed uniformly over the cathode surface. They rise due to
their buoyancy, but remain in the electrode sidewall boundary layer until they reach the
free surface. As they rise they are also convected downstream by the boundary-layer
flow, but more slowly than would be expected. As the current increased the gas genera-
tion rate increases, (see Eq. 13.) but the bubbles continue to move away from the
electrode surface such that voltage drop at the wall is not significantly effected

Comparison of Figs. 4 through 8 illustrates that the electrical characteristics of all of
the electrode materials tested are quite similar (with the exception of copper electrodes
which formed oxide films, Fig. 6b. The copper oxide films severely limit the current. All
other electrode materials exhibit linear variations of current density with applied electric
field. As might be expected each material had a somewhat different initiation voltage, $V_i$.
(i.e. the voltage or electric field which must be applied before appreciable current will
flow). The initiation voltage and "zero-current" electric field for each electrode pair
tested are summarized in Table 2.

The Eltech metal-oxide coated electrodes exhibited the highest $V_i$ of the electrodes
tested but there were no large differences between any of the electrodes. The values mea-
sured are consistent with the voltage drops measured in water electrolysis cells[14].

**Table 2.** Approximate electrode voltage drops

| Anode | Cathode | Initiation Voltage, volts | Zero Current Electric Field, volts/cm |
|---|---|---|---|
| Aluminum | Aluminum | ·5 | 0.3 |
| Incoloy 800 | Incoloy 800 | · · | 0.2 |
| Copper | Copper | ·5 | 0.3 |
| Eltech | Eltech | 2·· | 0.4 |
| Eltech | Hastelloy C | ·9 | 0.45 |

The flow velocity of the water through the channel was varied from about 6 to almost 90 cm/sec. In addition, some current/voltage data were obtained under static conditions. Comparison of Figs. 4 through 8 illustrate that for the range covered in these tests, changing the flow velocity did not alter the electrical characteristics in any significant way. Comparison of ... ith the data in Figs. 7 and 8 (see circle symbols in Figs. 7 and 8 corresponding to the start of the test series) illustrates that the E vs j data for velocities of 0, 20, 47 and 77 cm/sec are almost coincident when the differences of initiation voltage, $V_i$ are taken into account.

Data given in Figs. 4, 5, 6a, 7, and 8 for an open channel configuration having a free water surface, characterize the maximum current densities which may be expected in a seawater MHD propulsion unit, if the electric field shown by the figure is taken as the sum of the applied electrical field and the induced electric field $(\vec{V} \times \vec{B})$ in an MHD duct. Electrolysis effects however, can reduce the current flow. (1) Trapped $H_2$ bubbles and gas in a closed channel, (2) oxidation products on the anode and (3) the products of other chemical reactions on the cathode will reduce the current density at a given value of the electric field from the values shown in these Figures. The causes of reduced current are discussed in subsequent sections.

*Closed Channel Configuration*

Two constant-area closed channels which were fully submerged in the water flow were also investigated (see Fig 2(b)). For both channels the bottom wall was the cathode, the top wall the anode and the sidewalls (i.e., the B-walls) were made of electrically insulating material. Copper electrodes were tested first and then abandoned because copper oxide films which formed on the anode very quickly limited the current (see Fig. 6(b)). As a result, most of the closed channel data were obtained with channels having aluminium electrodes. The closed channel dimensions and test condition are presented in Table 3.

**Table 3.** Closed Channel Geometries

| Channel | Electrode Spacing, | Electrode Height | Electrode Length | Flow Velocity |
|---|---|---|---|---|
| | cm | cm | cm | cm/sec |
| (a) | 3.7 | 2.6 | 20.4 | 18 to 90 |
| (b) | 3.7 | 3.4 | 13.8 | 26 to 70 |

The channel flow was discharged into a diffuser with diverging sidewalls. For Channel (a) the top and bottom walls of the diffuser were parallel and horizontal. In later tests with Channel (b) the top diffuser wall was also diverged $2°$.

## CLOSED CHANNEL TESTS WITH HIGHER FLOW VELOCITIES

The variation of current density with electric field for the two closed channels is given in Fig. 9 when the channel flow velocities were 70 and 90 cm/sec. As occurred with the open-top channel the current density varied linearly with increasing electric field in the closed channel at these flow velocities. Comparison of the electrical characteristics of closed channels with aluminium electrodes (Fig. 9) to the electrical characteristics of the open-top channel with aluminum electrodes (Fig. 4) indicates that the closed channel had about the same initiation voltage $(V_I)$ as measured for the open-top channels, but at a given electric field the current densities in the completely closed channels were about 10% to 15% lower than measured in the open-top channel. The specific gravity and electrical conductivity of the simulated seawater were essentially the same for these two tests. This current decrease appears to be associated with the $H_2$ generation in the electrolysis process and represents a loss of performance in an MHD seawater thruster operating at these velocities. The cause of this current decrease is discussed fully in the section describing the observed bubble dynamics.

## CLOSED CHANNEL TESTS WITH LOWER FLOW VELOCITIES

### Channel (a) with a Horizontal Diffuser Top Wall

The current changed drastically when the water flow velocity was decreased. Figure 10 summarizes the time variation of the electrode current at two lower velocities (18 cm/sec and 34 cm/sec) for Channel (a) with a horizontal diffuser top wall. With the configuration of a horizontal diffuser top wall gas bubbles which are swept out of the channel rise to the top diffuser and become trapped against the top wall. Surface tension forces impede their movement downstream. As a result, large gas pockets were formed on the top diffuser wall which grew back upstream into the MHD channel. The consequence is that the trapped gas begins to cover part of the anode surface and causes the current to decrease. The gas pockets however do move slowly downstream and periodically escape from the diffuser exit. Thus, the channel-diffuser combination discharges $H_2$ gas pockets in a regular periodic fashion. When this occurs and a large pocket of gas escapes the current rises again to its initial value. Whereupon the current begins to again decrease as new gas pockets form.

As shown in Fig. 10, the period between $H_2$ gas discharges is quite regular. The period depends upon the level of the applied voltage and the flow velocity. Increasing the applied voltage increases the current flow and gas generation rate (see Eq. 13). This in turn decreases the period of the discharge (see Fig. 10b). Increasing the flow velocity at constant applied voltage more rapidly convects the gas bubbles downstream so that the gas pockets build more slowly which increases the period (compare Fig. 10a with the middle curve in Fig. 10b) A horizontal top wall diffuser in a seawater MHD thruster is clearly undesirable since it would result in a low frequency "fluctuation" of the thrust at low operational velocities. At channel velocities of 70 cm/sec and above current oscillations as shown in Fig. 10 did not occur. Moreover, they also may be eliminated by diverging the diffuser top wall as described below.

## Channel (b) with a Diverging Diffuser Top Wall

Channel (b) had the diffuser top wall diverged 2° (i.e. slanted upward). With this configuration the large gas pockets described above did not form along the diffuser top wall. Some $H_2$ gas bubbles coalesce forming larger bubbles but they move along the wall with sufficient velocity to prevent accumulation of large amounts of gas in the diffuser as occurred with a horizontal top wall. Consequently, the periodic discharge of gas pockets and the periodic variation of electrode current were eliminated.

The closed Channel (b) when operating at low velocity, however, exhibited a decrease in electrode current to a lower equilibrium value as shown in Fig. 11. The final equilibrium current level can be significantly less than currents achieved in the open-top channels and given previously in Figs. 4 to 8. The current decrease is again the result of bubbles or gas trapped on the electrodes (in this case the anode) as discussed in the next section. The time to reach the equilibrium current and the amount of the current decrease depends upon the flow velocity and the applied voltage (i.e., current level).

Thus, diverging the diffuser top wall eliminated the undesirable periodic discharge of gas in the flow channel. However, the longer residence time of the $H_2$ bubbles in the flow at lower velocity, decreases the current flow in a closed channel from what might be expected based upon the seawater conductivity (i.e., Figs. 4 to 8).

### Summary

Table 4 summarizes the degradation of current density which for these tests occurred in a closed channel as a result of $H_2$ gas formation in the electrolysis process. Values of the maximum current density achievable in an open-top channel are also shown for reference purposes:

**Table 4.** Summary of current density in closed channels at various operating conditions.

| | Electric Field, E, volts/cm | | |
|---|---|---|---|
| | 2.16 | 4.05 | 6.49 |
| *Velocity = 26 cm/sec* | | | |
| Initial Current Density amp/cm² | .068 | .138 | .220 |
| Final Equil. Current Density amp/cm² | .035 | .085 | .160 |
| Time to Reach Equil., min. | 7 | 3 | 2 |
| Max. Current Density Possible, amp/cm² | .082 | .158 | .270 |
| *Velocity = 70 cm/sec and above* | | | |
| Initial Current Density amp/cm² | .068 | .138 | .220 |
| Final Equil. Current Density amp/cm² | .060 | .130 | .220 |
| Time to Reach Equil., min.. | Nil | Nil | Nil |
| Max. Current Density Possible, amp/cm² | .082 | .158 | .270 |

These test results are shown in a different way by Fig. 12 which compares the variation of the measured current density with electric field for a closed channel (cathode on the bottom wall) with the measurements for an open channel. This comparison illustrates that due to $H_2$ gas formation in the electrolysis process a higher applied voltage will be necessary to achieve a given current and hence propulsive thrust in a closed channel than would be ideally expected from the value of the seawater electrical conductivity. Because the channel flow velocities for these tests were much lower than would exist in a typical

seawater thruster, there is a tendency to believe that this potential loss of performance will be greatly reduced and perhaps eliminated as flow velocities increase. However, the observations of bubble dynamics described in the next section clearly suggest that the current losses are due to the bubbles that move through low-velocity sidewall boundary-layer regions because of their buoyancy. They accumulate in the upper corner between and electrode and the sidewall and result in blocking a part of the electrode surface area. Simply increasing the overall flow velocity may not significantly alter the mechanisms which results in gas accumulation at the electrodes.

## BUBBLE DYNAMICS

As shown by Figs. 4 through 12 four modes of current flow were observed during these tests:

(1) A linear variation of current with voltage, with current levels corresponding to the ideal values expected for the salt water specific gravity and electrical conductivity. This result occurred in an open-top channel with a free surface and the electrodes served as the vertical sidewalls which allowed the $H_2$ to escape.

(2) A linear variation of current with voltage for a closed channel but with currents about 10% lower than the ideal value. This result occurred when the closed channel velocity was 70 cm/sec or greater.

(3) A periodic fluctuating current in a closed channel at velocities below about 40 cm/sec and with a horizontal top wall on the diffuser.

(4) A significantly decreased but steady current in a closed channel at velocities below about 40 cm/sec and with a $2^{\circ}$ diverging top wall on the diffuser.

All of these current modes were a function of gas generation rate in the channel and the bubble dynamics.

*Open-Top Channel Bubble Dynamics*

Observation of the bubble formation in the open-top channels clearly demonstrate that small diameter bubbles (probably less than 0.5mm in diameter) are generated uniformly over the cathode sidewall and to a lesser degree on some anodes (the Eltech material and aluminum for example). The bubbles rise and move downstream in the electrode sidewall boundary layers under a balance of forces due to (1) shear in the boundary layer, (2) their natural buoyancy and (3) their surface tension with the wall. As they reach the water surface they coalesce into much larger bubbles and either escape from the free surface into the atmosphere or float downstream on the surface and along the wall forming a "foam boundary layer". In any event with a free-surface the bubbles do not appear to move out of the sidewall boundary layers where they are generated and into the free-stream except when they reach the free surface. Figure 13(a) is a photograph of bubbles formed in an open-top channel. It illustrates (1) the layer of small bubbles forming on the cathode surface, (2) the foam boundary layer at the free surface and (3) the absence of any bubbles in the free stream. A sketch of the bubble dynamics with this configuration is given by Fig. 13(b). The bubble formation and their movement does not significantly impact the electrical characteristics. At a given applied voltage the current that results is what would be expected from the conductivity of the water.

## Closed Channel Bubble Dynamics

In a closed channel the situation is different. Some of the gas that is generated at the top wall or rises through the sidewall boundary layers tends to be trapped against the top wall. Surface tension forces are enhanced on the top surface since the buoyant force pushes the bubble against the top wall. Shear forces in the top wall boundary layer are not sufficient to move the gas downstream very rapidly.

One brief test was conducted with a closed channel having the cathode as the top wall. Hydrogen generated at the cathode became trapped against the cathode surface due to its buoyancy and surface tension. This greatly reduced the current which could be passed through the seawater. No data were taken for this configuration because it didn't appear to be of practical interest. For all other closed channel tests the cathode was placed on the bottom wall and the anode served as the top wall. With this orientation most of the hydrogen produced at the cathode will rise through the cathode boundary layer because of its buoyancy and move into the free stream (see Fig. 14(a)).

Acoustic measurements, to be reported in later work, suggest that the size of the bubbles generated in these tests was in the range between 0.1 to 0.5 mm in diameter. This size range was also consistent with visual observations. Bubbles of this size will have a rise velocity between 1.5 and 5 cm/sec.[15] Assuming that the bubbles are spherical, they are subject to a vertical buoyant force ($F_B$) and a drag force ($F_D$) moving them horizontally. It can be easily shown that the ratio of $F_B$ to $F_D$ for "free" bubble is:

$$\frac{F_B}{F_D} = \frac{gD}{3C_D^2 V}$$

(15)

where $D$ is the diameter of the bubble, $C_D$ is the drag coefficient for a sphere (which depends on Reynolds number), $V$ is the flow velocity, and $g$ is the acceleration due to gravity. For the conditions of these tests the ratio:

$$\frac{F_B}{F_D} \ll 0.1$$

Thus, the bubbles rising out of the cathode boundary layer and into moving the free stream (which had a velocity as high as 70 to 90 cm/sec) are sweep downstream and out of the channel before they could rise to the top of the channel, (see Fig. 14(a)). Even at the lower velocities of these tests (near 20 to 30 cm/sec), a large portion of the bubbles generated on the bottom wall are swept out of the channel before rising to the top wall.

The situation is different however for bubbles formed at the cathode and sidewall corner. These bubbles will rise in the sidewall boundary layer and stay close to the side-wall. As a result many of these "boundary layer" bubbles reach the top before moving out of the channel since in this case:

$$\frac{F_B}{F_D} = O(1) \tag{16}$$

The migration of bubbles generated in the bottom corners is also sketched in Fig. 14(a). Bubbles which rise through the sidewall boundary layers create small gas pockets at the corners between the sidewalls and the anode. The effect of these gas pockets is to reduce the effective surface area of the anode and reduce the current flow. This bubble flow pattern is responsible for the decrease in current measured for the closed channel operating at higher velocities. (Compare Fig. 9 with Fig. 4 or see Fig. 10)

As the channel flow velocity decreases, this effect becomes more pronounced; moreover, at the lower flow velocities some of the gas generated at the bottom of the channel may rise to the anode before leaving the channel and block even more of the anode. This bubble behavior produces the larger current decrease with time as shown in Fig. 11 for a low channel velocity.

Gas generated at the floor of the channel and swept into the diffuser can then rise further and be trapped against the diffuser top wall. When that wall was horizontal, large gas pockets accumulated which as outlined earlier cause the periodic fluctuation in current summarized in Fig. 10.

## IMPLICATIONS FOR A SEAWATER THRUSTER DESIGN

The results of these tests (even though the scale and velocities were small) suggest potential performance problems with seawater MHD thrusters which will have to be considered. In addition, they also suggest channel geometries and orientations which may be more desirable.

### Effect of Bubble Formation on Channel Performance

These tests have indicated a 10 to 15% reduction of current densities in closed channels having flow velocities as high as 90 cm/sec (see Fig. 12) due to bubble-induced gas blockage at the electrode. The end effect of the gas blockage in the channel is to reduce the electrical efficiency of a seawater MHD propulsion unit.

A simple analytical model which approximates the performance of an MHD seawater thruster has been developed by Bagley* at DTRC. As an example, a particular calculation, using his model to estimate the performance of a ship MHD propulsion unit having a magnetic field of 5 tesla and a current density of 0.2 amp/cm$^2$, indicated a thruster electrical efficiency (the ratio of MHD power out to electrical power in) of about 24.3%. If 13% of the electrode surface area is blocked by a gas sheath, which is the reduction indicated by the Fig. 12 data, the thruster electrical efficiency would decrease to 21.8%. It should be emphasized that these values are approximate and that the scale and velocities used in these tests may cause a greater degradation of current than may occur in a full-scale configuration. Moreover, a complete MHD channel will produce the Lorentz force $(\vec{j} \times \vec{B})$ in the fluid and in the boundary layer which may act to move the bubbles in the boundary layer downstream more rapidly. This force on the fluid was absent in these

---

* Bagley, David E., private communication (Sep 1989).

tests since $\vec{B} = 0$. However, the potential for decreased performance due to gas bubbles and/or gas pockets on the electrodes should not be dismissed lightly.

*Channel Configuration*

The observation of the $H_2$ bubble dynamics and the measurement of their effects provide some guide to the design of an MHD thruster. First, it would appear highly desirable to avoid horizontal or converging channel top walls (ceilings) in flow passages where $H_2$ bubble may exist which tends to trap bubbles due to surface tension effects and allows gas pockets to form. This suggestion would apply to the diffuser as well as the channel. Diverging the channel walls and particularly the top wall should decrease or minimize current losses due to gas blockage.

For a linear MHD channel it appears desirable to place the cathode at the bottom of the channel. (see Fig. 14(a). This should maximize the possibility of the bubbles getting into the free stream and being swept out of the channel before rising to the top electrode where they would provide a high-resistance blockage to the current flow. Since some anode materials produce less gas than others, their use would also be desirable. As outlined later, those anodes which demonstrated good durability, however, also produced gas on the anode surface.

If the electrodes are at the sidewalls of a linear channel, larger amounts of the $H_2$ gas may be trapped in the boundary layers as illustrated in Fig. 14(b). These tests suggest that a linear channel with electrode sidewalls may inherently have lower performance unless some means is provided to remove the bubbles or gas pockets, or unless the flow velocity is high.

The concept of an annular MHD propulsion unit configuration which is wrapped around the hull of a submerged vehicle has been suggested several times over the past twenty-five years.[2, 16, 17] This configuration has a number of advantages related to (1) a simpler magnet design and (2) minimizing the size and perhaps cost of the MHD propulsion unit appendage which would have to be added to a conventional submerged vehicle hull. A sketch of this configuration is shown in Fig. 15(a).

It's not yet clear how the outer annulus wall would be structurally supported. This sketch shows that the outer wall is supported by vanes in the inlet nozzle and exit diffuser which would enclose part of the magnet coil windings. The azimuthal magnetic field would be provided by several coils which would be enclosed in the outer wall, the end support vanes and then the inner wall. This arrangement would leave an unobstructed annular MHD flow passage as shown in Fig. 15(b). Such an arrangement would minimize the formation of $H_2$ gas pockets being trapped in the MHD channel and interfering with the current flow if, as sketched in the figure, the inner wall served as the cathode. Gas formed at the inner electrode would escape into the free steam and be swept out of the channel before reaching the outer electrode. Thus, this arrangement would appear to be much less susceptible to current losses due to gas blockage effects described above.

If, however, it would become necessary to provide support walls over the length of the MHD channel between the inner body (the cathode) and the outer body (the anode), the annular passage would be partitioned or segmented. Should structural consideration make such support partitions necessary, or that it is done to subdivide the thruster for directional control purposes, the electrodes in each sector would be oriented in different

directions with respect to the direction of the gravitation force. The observation of $H_2$ bubble dynamics in these tests and the tendency of the bubbles to remain in the low-velocity boundary layers suggest that the problem of trapped gases interfering with the current flow in some of the thruster segments could be a problem with this configuration. The efficiency of the thruster would be reduced and should this occur, the thrust form each sector to the MHD propulsor could vary considerably. The end effect would appear to be a force couple acting in the nose-down direction.

## LONG DURATION TESTS

Two long-duration electrode tests were carried out to obtain information concerning the durability of some electrode materials and to gain some insight into the operation of closed-loop facilities designed to evaluate seawater MHD thrusters. A 50-hour accumulative test was made with Electrode Pair 4 DSA® (Eltech Anode* and DSA® Eltech Cathode) and 100 hours of operation of Electrode Pair 5 DSA®(Eltech Anode and Hastelloy C Cathode) was carried out.

### 50-Hour Test of Eltech Electrodes*

Figure 7 summarizes the current/voltage characteristics of an Eltech anode and cathode combination with over 50 hours of testing at an electric field of 6 volts/cm and a current density of approximately 0.25 amp/cm$^2$. There were no important changes of the electrical characteristics over the course of the tests. Changes in current at a given voltage shown in Fig. 7 were due to (1) increase of the water temperature during the run and (2) the formation of magnesium or calcium scaling products on the anode. Moreover, there was no visible or measurable degradation of the electrode surfaces over the 50-hour test.

### Effect of Water Temperature

This 50-hour test was made up of several 6 to 10 hour continuous runs. Over the course of the run, energy is added to the water by the circulating pump and by the current passing between the electrodes and through the water. As a consequence, the temperature of the water rises a few degrees over the run. The electrical conductivity of the simulated seawater is relatively sensitive to the water temperature. Figure 16 shows the variation of current with time for the constant applied voltage of 30 volts. During a run the current rises as the water temperature rises. Then, overnight the facility was shut down and the water temperature returned close to its original value. This cycling or variation of water temperature with time resulted in the sawtoothed current history given in Fig. 16. With constant values of applied voltage, flow velocity, specific gravity of the water and channel geometry, it was possible to measure the resulting current at temperatures between about 65°F to 92°F. As illustrated by Fig. 17, a 25°F temperature variation resulted in about a 25% change in current. Consequently, one must exercise care in interpreting current data in a closed MHD thruster test facility in which the water or electrolyte temperature can change. Since the current varies linearly with water (electrolyte) temperature, it would be simple to correct current data for changes in the water temperature.

### Effect of Scaling Products at the Cathode

As noted earlier the very high pH condition which exists at the cathode results in the formation of magnesium and/or calcium hydroxide. This material is glantinous and ad-

* See footnote for Table 1 for information related to these electrodes.

hered to the cathode surface. Some observations over the course of the tests concerning these deposits are made in Fig. 18. While these scale deposits were wiped from the cathode between most of the run periods, they did nevertheless form a crust on the cathode surface as the test progressed as shown by Fig. 19.

This cathode scaling material $Ca(OH)_2$ and $Mg(OH)_2$ is electrically insulating. So, as the $Mg(OH)_2$ and $Ca(OH)_2$ scale accumulates on the cathode over a period time, it reduces the current. This effect can be seen in Fig. 16 by the decrease of the initial current at the start of each run period from the start of the test, up to a total run time of about 36.6 hours (i.e., the dash-dot line). Current data taken from Fig 16 is summarized in Table 5.

Table 5. Current variation with time for long-duration tests.

| Accumulated Test Time, hr | Current (T = 70°F), amp |
|---|---|
| 0 | 5.6 |
| 7.6 | 5.44 |
| 15.7 | 5.17 |
| 25.0 | 5.17 |
| 36.6 | 4.93 |
| 44.2 | 5.59 |
| 50.5 | 5.44 |

At an accumulated run time of 44.2 hours the cathode was removed from the channel, scrapped clean, re-installed and run for a short time with reversed polarity. Running the cathode as an anode for a short time effectively removed the scale. With the cleaned cathode, Fig. 16 illustrates that the current increased to nearly the level measured when the cathode was new. Continuing to run the cathode for another 6.3 hours resulted in the current beginning to again decrease as more scale formed. Appendix A provides a chemical analysis of this scale material.

*Other Long Duration Trends*

Figure 18 summarizes the cathode and anode weights over the 50 hour test period. The cathode exhibited a slow weight increase as a scale crust accumulated. When the electrode polarity was reversed and the scale removed, the cathode weight returned to its original value. The weight of the anode appeared to vary slightly over the course of the test. The weight changes shown in Fig. 18 are believed to be due different moisture contents of the oxide coating since the electrodes were just wiped dry and weighed. It is believed that the 50-hour test did not result in any measurable weight loss for either the Eltech anode or cathode.

The electrolyte pH was also recorded over the period of this test (see Fig 18(b)). The pH was observed to rise initially over the first few hours of the test as hypochlorite ions were produced. After that it continued to increase but rather slowly. It should so be noted that the slight odor of $Cl_2$ was present over the free-surface of the water form time to time when the electrodes were powered. Measurements just over the surface of the wa-

ter and near the channel indicated $Cl_2$ concentrations of 3 to 5 ppm which is the level of its odor threshold. This electrolysis process did not generate any appreciable amount of free $Cl_2$.

*100-Hour Test of Eltech/Hastelloy Electrodes*

Tests of the stainless steel Electrode Pair 3 indicated that the $Mg(OH)_2$ and $Ca(OH)_2$ scaling products did not adhere as readily to the electrode surface. Moreover, discussions with others* indicated that commercially available electrolysis cells utilize stainless cathodes to reduce the scaling problem. For these reasons, a 100-hour test of a polished Hastelloy C cathode and an Eltech DSA$^®$ anode was made. This test consisted of several 8-hour to 24-hour continuous run periods. The purposes of the test were to (1) gain information about the durability of this electrode pair, (2) to observe the location and amount of scaling and (3) measure the electrical characteristics of this electrode pair. (Fig. 8)

*Scale Formation*

The magnesium/calcium scale formed near the cathode surface but it did not adhere to the polished steel surface to any important degree. At the entrance and exit of the channel, however, there were vertical wall seams where the channel was butted to the nozzle exit and diffuser entrance. These vertical seams on the cathode side of the channel represented small but finite wall discontinuities. Scaling products become attached to these discontinuities and grew upstream on the nozzle sidewall and downstream on the diffuser sidewall. They also grew outward from the wall in the form of a vane-like bulge that extended well beyond the wall boundary layer. The flow velocity was 77 cm/sec for these tests. The $Ca(OH)_2/Mg(OH)_2$ scale products also grew in the corner between the cathode sidewall and channel floor where velocities were relatively low and then outward across the channel floor to the anode. It primarily adhered to the floor rather than the cathode.

For the channel size and flow velocity of these tests the growth of the $Ca(OH)_2$ and $Mg(OH)_2$ scale was sufficient to create disturbance and blockage of the flow. After one 24-hour continuous run period the scaling material was collected from the nozzle/channel/diffuser walls and weighed, after it had been dried. During this test period the weight of the scale accumulation was about 0.22 gms per square centimeter of cathode surface area. This corresponds to an accumulation rate in the channel region of roughly:

$$m = 0.01 \text{ gm/hr/cm}^2 \text{ of cathode area}$$

After 100 hours of running the scale material coated most of the wetted surfaces in the test facility to some degree.

The use of a polished stainless steel cathode greatly minimize the formation of the scale material on the cathode surface. Moreover, the use of these electrodes almost eliminates the current reduction and loss of MHD channel performance due to scaling which occurred with an Eltech or aluminum cathode. However, the production of the magnesium and perhaps calcium oxides at the cathode may cause some losses of channel performance by creating blockage and flow disturbances which may lead to higher pressure drops in the exit diffuser. In addition, this material may cause some operational problems in closed-loop test facilities where it can accumulate and initiate disturbance to the flow. This may be particularly important in facilities where acoustic testing of MHD thrusters is to be done.

---

* Niksa, M., Eltech Corp., private communication (June 1989).

This electrode pair accumulated 109 hours run time at a current density of 0.30 amp/cm². A summary of the test periods is given in Table 6. The performance of both the anode and cathode over this period was excellent.

**Table 6.** Summary for 100 hour test

| Date | Power On | Power Off | Run Time, hr | Total Time, hr |
|------|----------|-----------|--------------|----------------|
| 9/7/89 | 9:35 am | 8:20 pm | 10.75 | 10.75 |
| 9/8/89 | 8:15 am | | | |
| 9/9/89 | | 9:35 am | 25.25 | 36.0 |
| 9/9/89 | 9:50 am | 5:50 pm | 8.0 | 44.0 |
| 9/11/89 | 8:50 am | | | |
| 9/12/89 | | 7:05 am | 22.25 | 66.25 |
| 9/12/89 | 7:05 am | | | |
| 9/13/89 | | 2:00 am* | 15.1 | 81.35 |
| 9/13/89 | 7:25 am | 6:50 pm | 11.25 | 92.60 |
| 9/14/89 | 8:45 am | 10:35 pm | 14.8 | 107.40 |
| 9/15/89 | 8:45 am | 10:45 am | 2.0 | 109.4 |

*Anode power supply connection failed at about 2:00 am.

Both electrodes were weighed before and after the 100 hour test. There were no significant weight changes.

## SUMMARY AND CONCLUSIONS

Systematic tests of the seawater electrolysis process in an MHD type channel have been carried out. There was no applied magnetic field for these tests and the Lorentz force on the simulated seawater was absent. The current/voltage or current density/electrical field characteristics measured during these tests are similar to those which will occur in an MHD seawater thruster, if the electric field for these tests is taken to represent the sum of the applied field and induced field in an MHD channel. These tests have led to the following conclusions:

1. The product Instant Ocean can be used to produce a test medium for MHD thruster tests which has the same electrical conductivity and specific gravity relationship as sea water (i.e. $\sigma = 4.5$ S/m and S.G. $= 1.024$). This product can also be employed to increase the electrical conductivity of the test medium to at least 10 S/m, if it is desirable to evaluate a seawater MHD thruster over a wider range of MHD conditions.

2. The current or alternatively the current density with a seawater electrolyte vary linearly with applied voltage or electric field up to a current density of at least 0.3 amp/cm² when there is the means to remove the hydrogen bubbles generated at the electrodes (principally $H_2$ at the cathode). An electrode voltage drop of 1 to 2 volts occurs and may be thought of as an initation voltage which must be applied before significant current will flow in the seawater electrolyte.

3. When the channel completely encloses the flow, $H_2$ gas generated at the electrodes can become trapped in the boundary layers. It rises to the top of the channel due to its buoyancy and forms pockets of gas. These gas pockets can, to a varying degree depending upon the orientation of the electrodes, cover a portion of the electrode surface and reduce the current flow. In this case the gas acts as an insulating sheath over a part of the electrode and reduces the MHD thruster performance. For the flow velocities these tests show that the loss of electrical current was at least 10 to 15% and as high as 50%. The current reduction should be less at higher flow velocities.

4. At low channel velocities the current varied periodically with time for test configurations with horizontal top walls (ceilings) in the channel and diffuser as the channel periodically discharged pockets of gas which had become trapped at the top surface.

5. Consideration must be given to the geometric design of a seawater MHD thruster and its exit diffuser to avoid the formation of pockets of trapped $H_2$ gas and/or to provide the means to remove the gas. Diverging top walls for the channel and diffuser may be necesseary for linear MHD thrusters in order to minimize gas blockage of the electrodes. The toroidal or annular MHD thruster configuration may have a configurational advantage in minimizing gas blockage, as long as it does not have to be portioned into segments. If, however, structural considerations dictate subdividing the annular passages into segments, to support the outer annular wall, some segments of the annular flow passage will in all likelihood have significantly reduced current. This would result in uneven thrust for the annular segments which is undesirable.

6. Copper and aluminum anodes were severely eroded as copper and aluminum oxides or chlorides formed. Moreover, the oxide or chloride film which quickly formed on the copper anode limited the current flow. Corrosion of other copper and aluminum materials used in the test facility was also rather severe. Stainless anodes were also oxidized, but to a lesser degree. Anodes (manufactured by Eltech Corp) proved to be durable in a 50-hour and 100-hour test. Under the conditions of these long-duration tests there was no visible or measurable loss of this anode material. These electrodes are designated by Eltech as DSA® (Dimensional Stable Anode) and are made up of a mixed metal oxide coating on a metallic substrate.

7. The principle problem at the cathode was the formation of a white gelanteous material from the salts in the electrolyte solution. The primary substance that formed during these tests was calcium or magnesium hydroxide. This material formed at the high pH condition at the cathode and adhered to the aluminum and Eltech cathodes. Since it is an electrical insulator, it reduced the current flow as it accumulates over long run times. This material could be easily removed by reversing the polarity. The $Mg(OH)_2$ and $Ca(OH)_2$ did not adhere as readily to two types of stainless steel electrodes which were tested. However, it did stick to and grow out from the nozzle, and diffuser walls as well as the insulated B-walls in regions where there were wall discontinuities and/or corners with low flow velocities.

8. An electrode pair made up of an Eltech anode (to minimize anode erosion) and a polished Hastelloy C cathode (to minimize the buildup of hydroxide scale films exhibited good performance over a 100 hour test at a current density of about 0.3 amp/cm$^2$. Following this test there was no measurable loss or visual damage to either electrode. However, while the $Ca(OH)_2$/ $Mg(OH)_2$ deposits did not form on the polished stainless cathode sur-

face, these deposits did form in other parts of the flow channel to the point of creating significant flow disturbances. At the low velocities of these tests this electrode pair, El-tech anode and a polished stainless cathode, appears promising for use in MHD seawater thrusters.

9. From the results of these tests it appears that it will be necessary to consider and control the formation of $Ca(OH)_2$, $Mg(OH)_2$ and other compounds in the flow inlet nozzle and exit diffuser adjacent to the cathode surface. In addition, MHD thruster test facilities will have the problem of an accumulation of these materials throughout the test facility particularly in corners or other flow regions where velocities are low and/or flow discontinuities exist.

10. With the use of the Eltech anode, hypochlorite ions $(ClO)^-$ form at the anode in which the $Cl_2$ produced at the anode is hydrolized to produce additional $H_2$. This will have the effect of slowly increasing the pH of the seawater test medium in a closed MHD thruster test facility. In addition, in a closed test facility the temperature of the test medium will also increase with time as energy is added to the water by (1) joule heating of the electrolyte and (2) a circulating pump. The electrical conductivity of the seawater is quite sensitive to water temperature. As a result, the electrical conductivity of the test fluid and as a result the current at a given voltage will increase with time as the electrolyte temperature rises. A temperature correction to the current/voltage data taken over long runs will probably be necessary.

## ACKNOWLEDGEMENTS
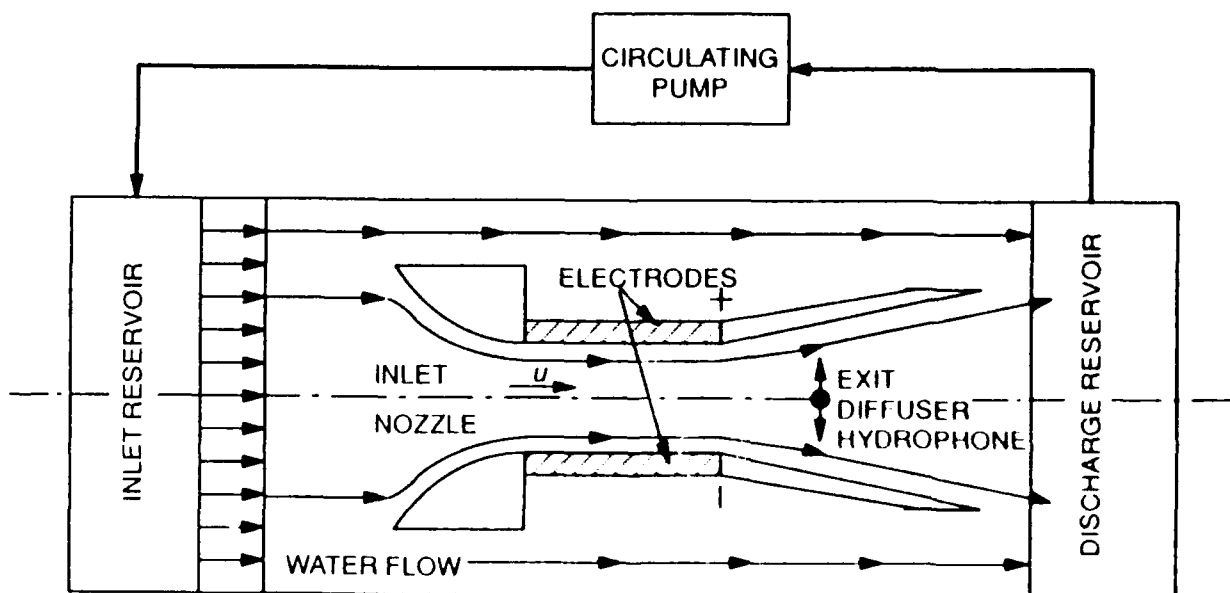
**Fig. 1.** Schematic of the test set-up for the open-top channel tests.
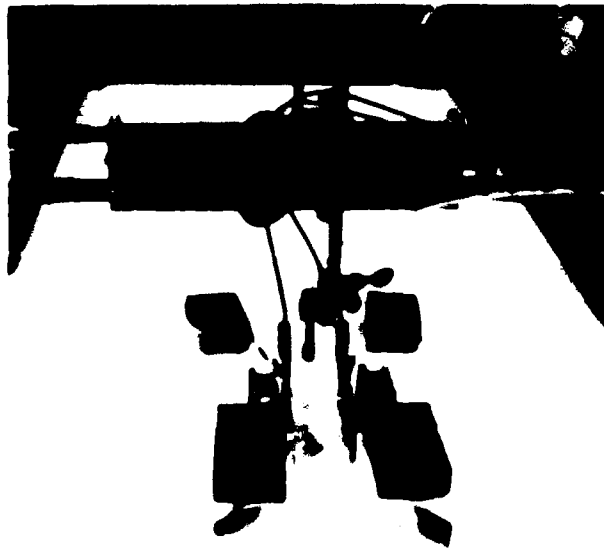
**Fig. 2a.** Open-top channel.
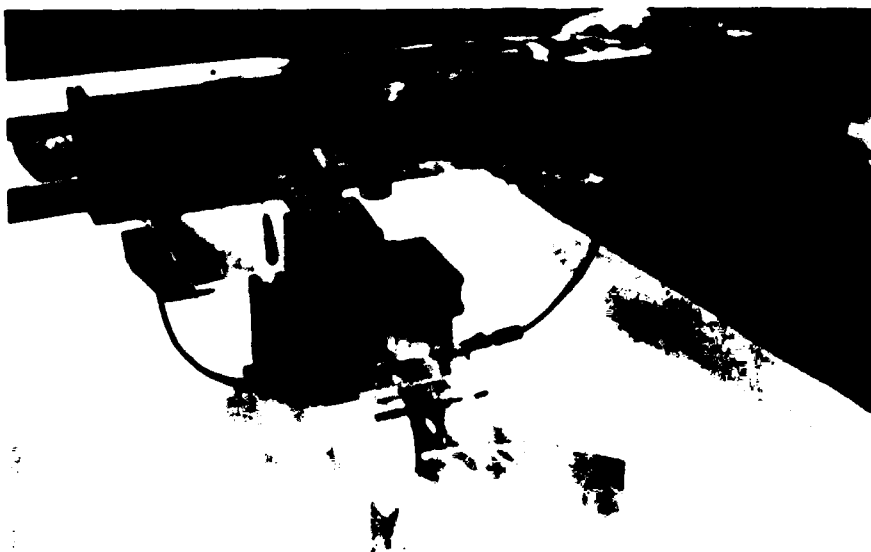


**Fig. 2b.** Fully enclosed channel.

**Fig. 2.** Open-top and closed channel configurations.
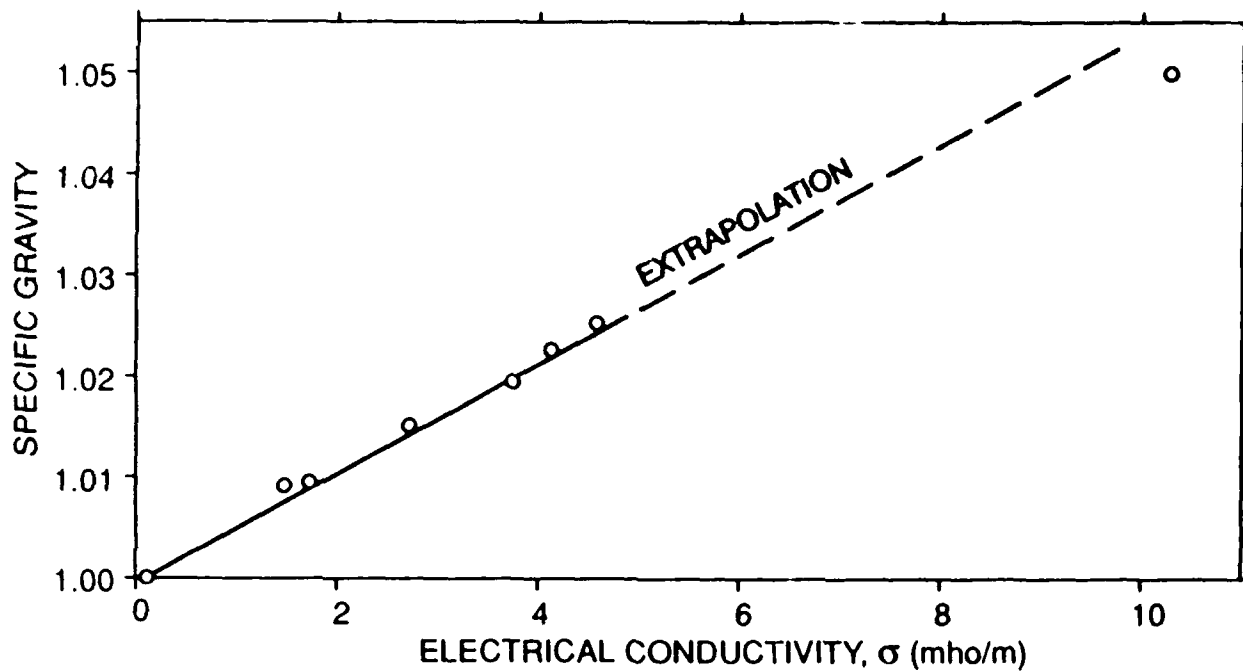
**Fig. 3.** Variation of measured electrical conductivity with specific gravity for simulated sea water.
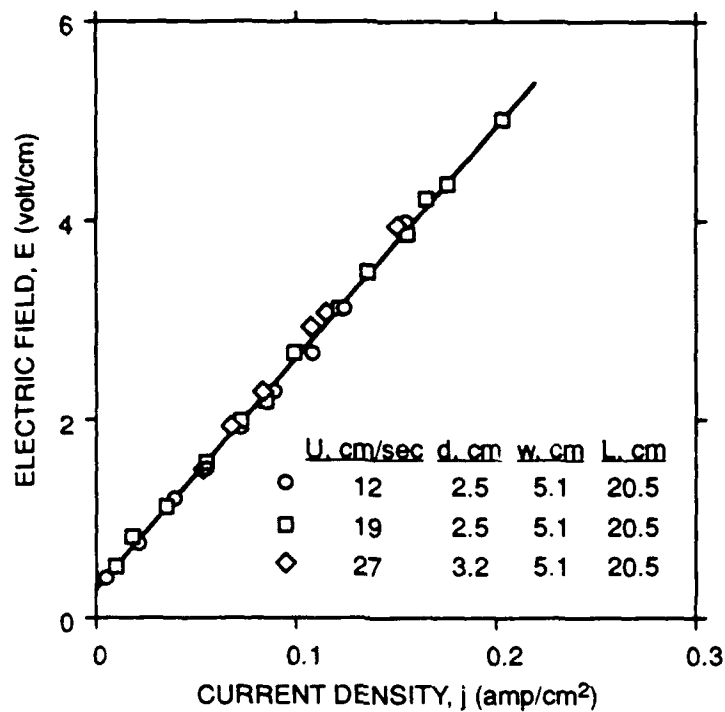


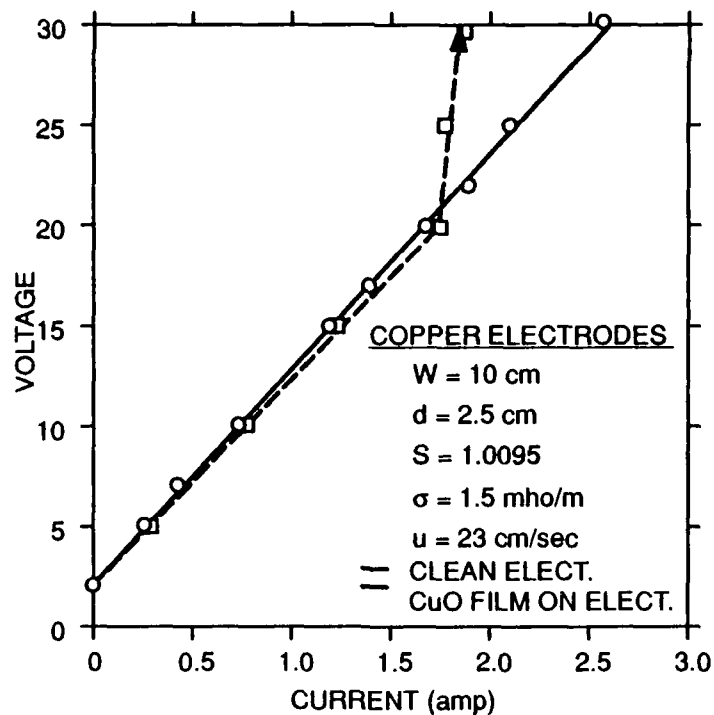**Fig. 4.** Current density variation with electric field for aluminum electrodes and different channel geometries.
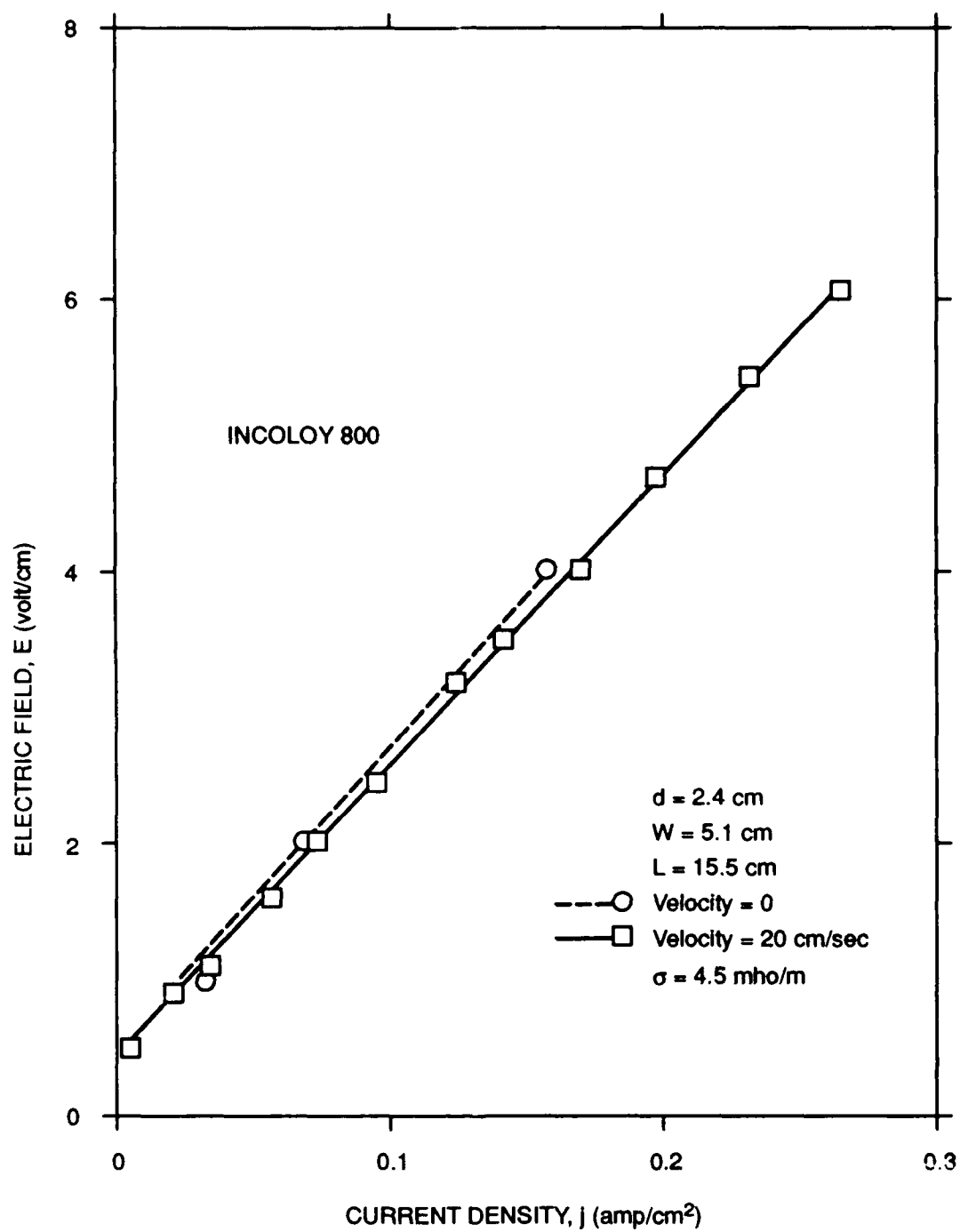
**Fig. 5.** Current density variation with electric field for Incoloy 800 electrodes at zero velocity and at 20 cm/sec.
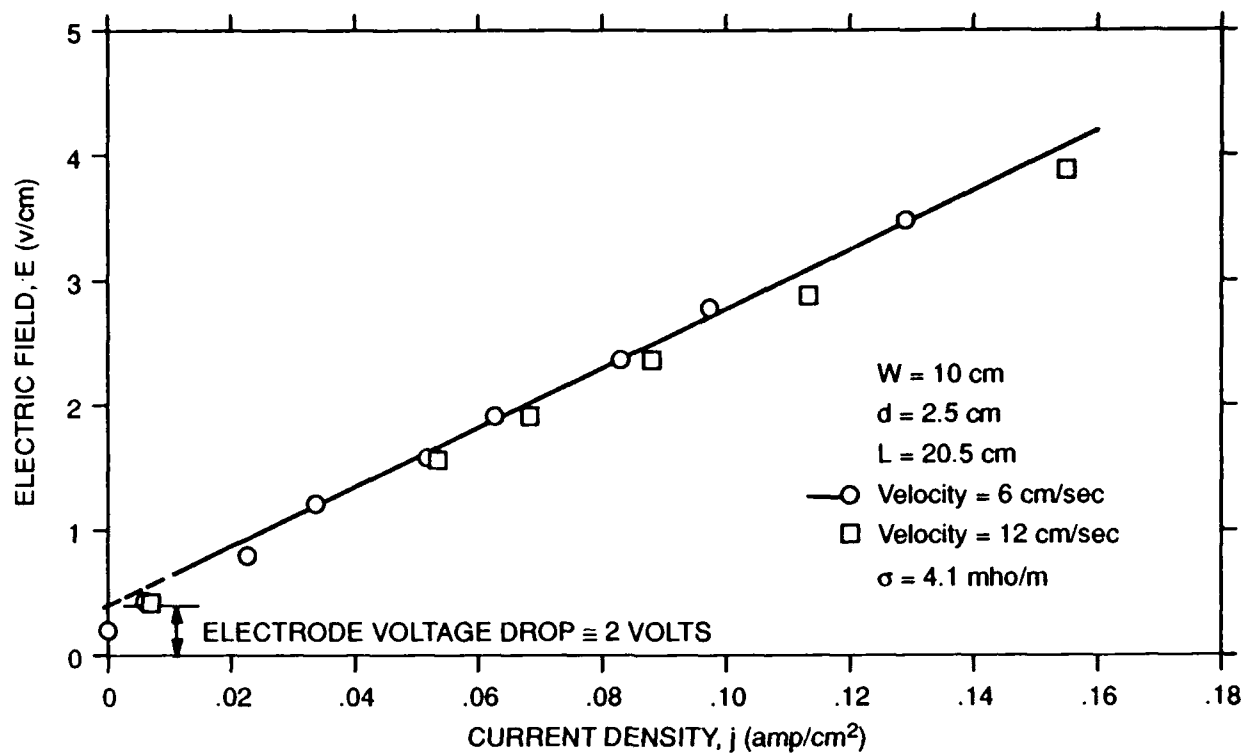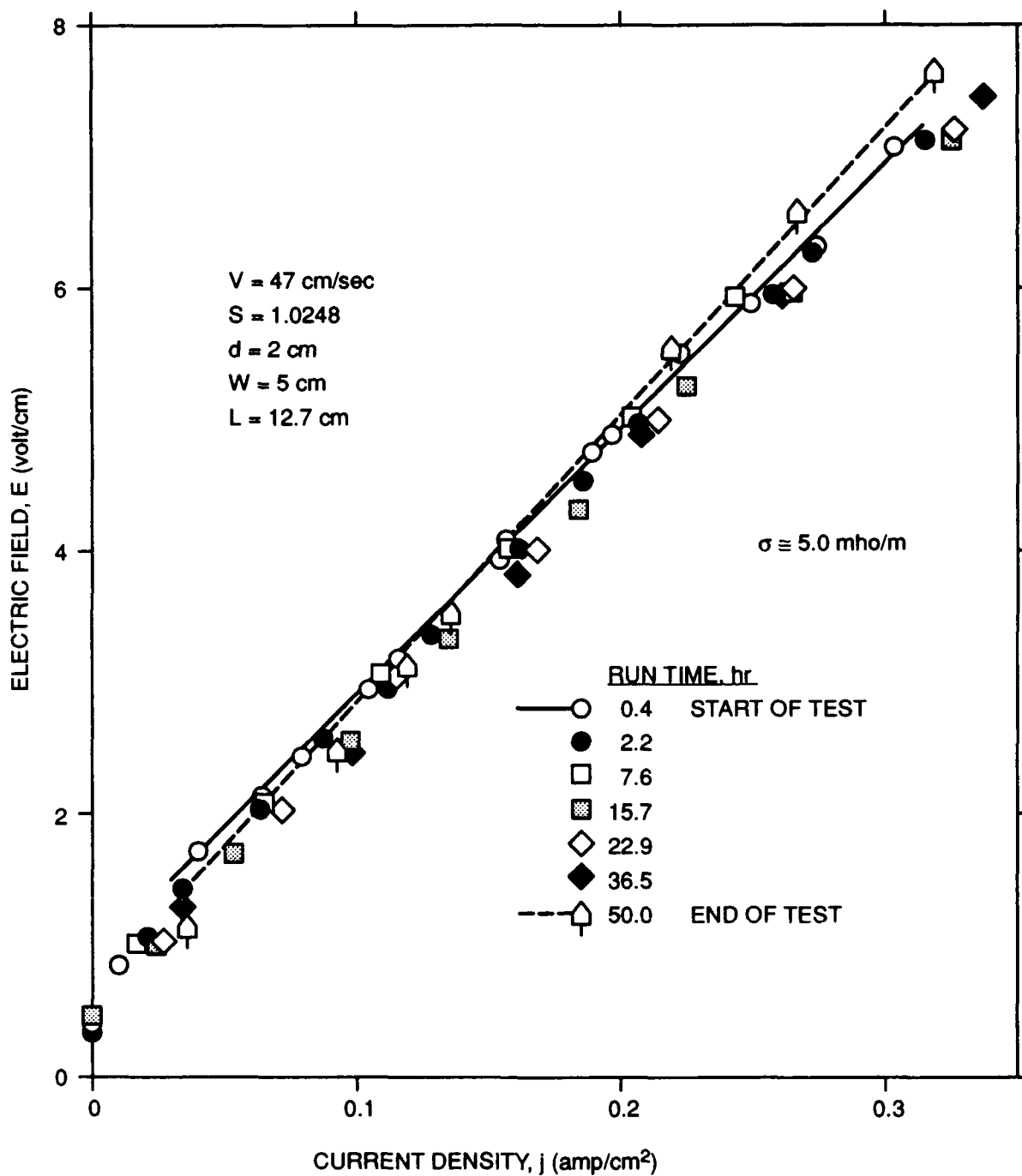
(a) Current density variation with electric field with clean electrodes.



(b) Effect of copper oxide corrosion film on anode suface.

**Fig. 6.** Electric characteristics of copper electrodes in an open-top channel

**Fig. 7.** Current density variation with electric field for Eltech DSA®
electrodes (mixed metal oxide coating on a metallic substrate).

ELTECH – ANODE
HASTELLOY – CATHODE
$V \cong 75$ cm/sec

——○—— T = 88°F   TIME = 0

□   T = 88°F   TIME = 11 hr

– – ◇ – –   T = 92°F   TIME = 44 hr

ELECTRIC FIELD, E (volt/cm)

CURRENT DENSITY, j (amp/cm$^2$)
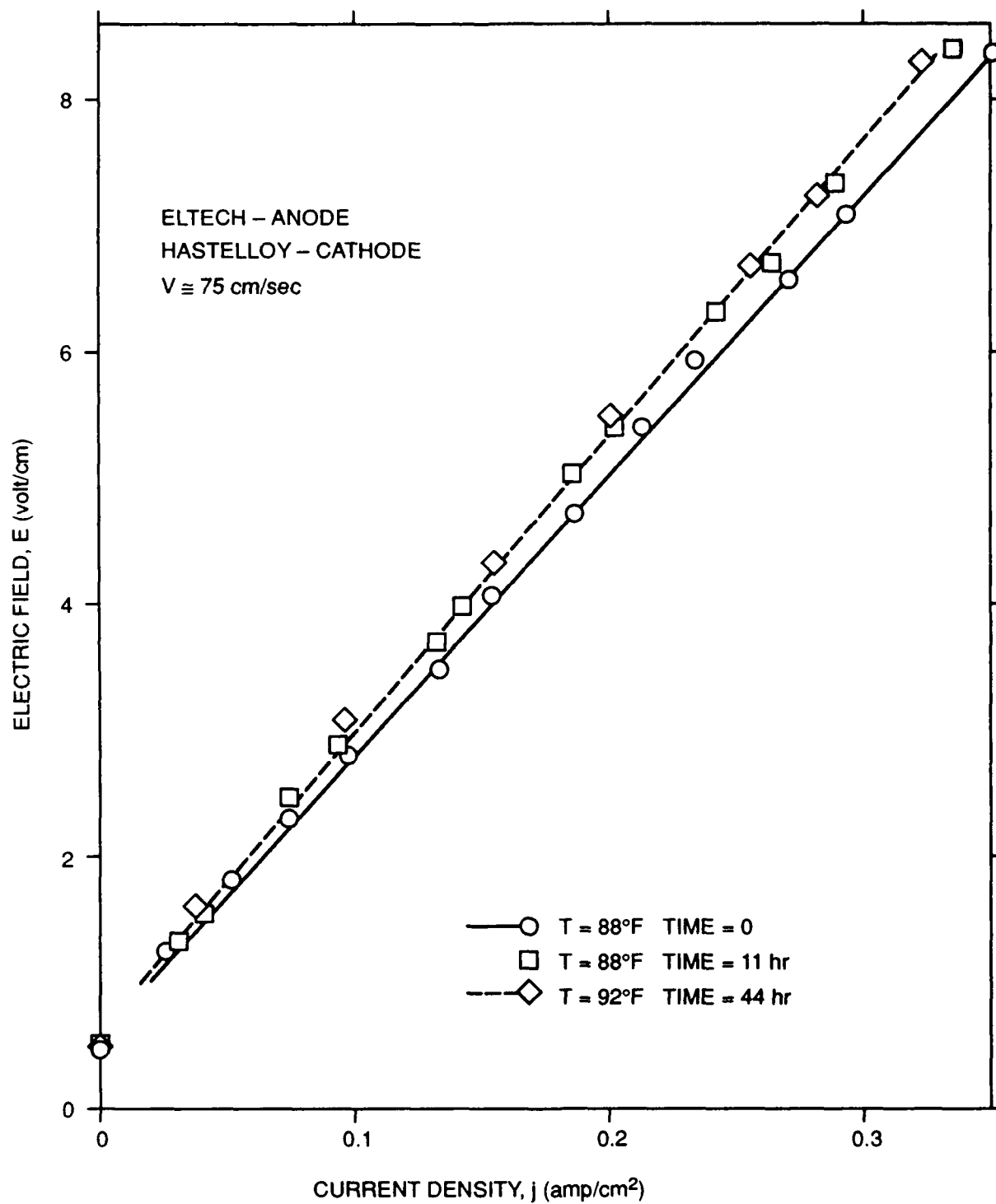
**Fig. 8.** Current density variation with electric field for an Eltech DSA® anode and a Hastelloy C cathode.
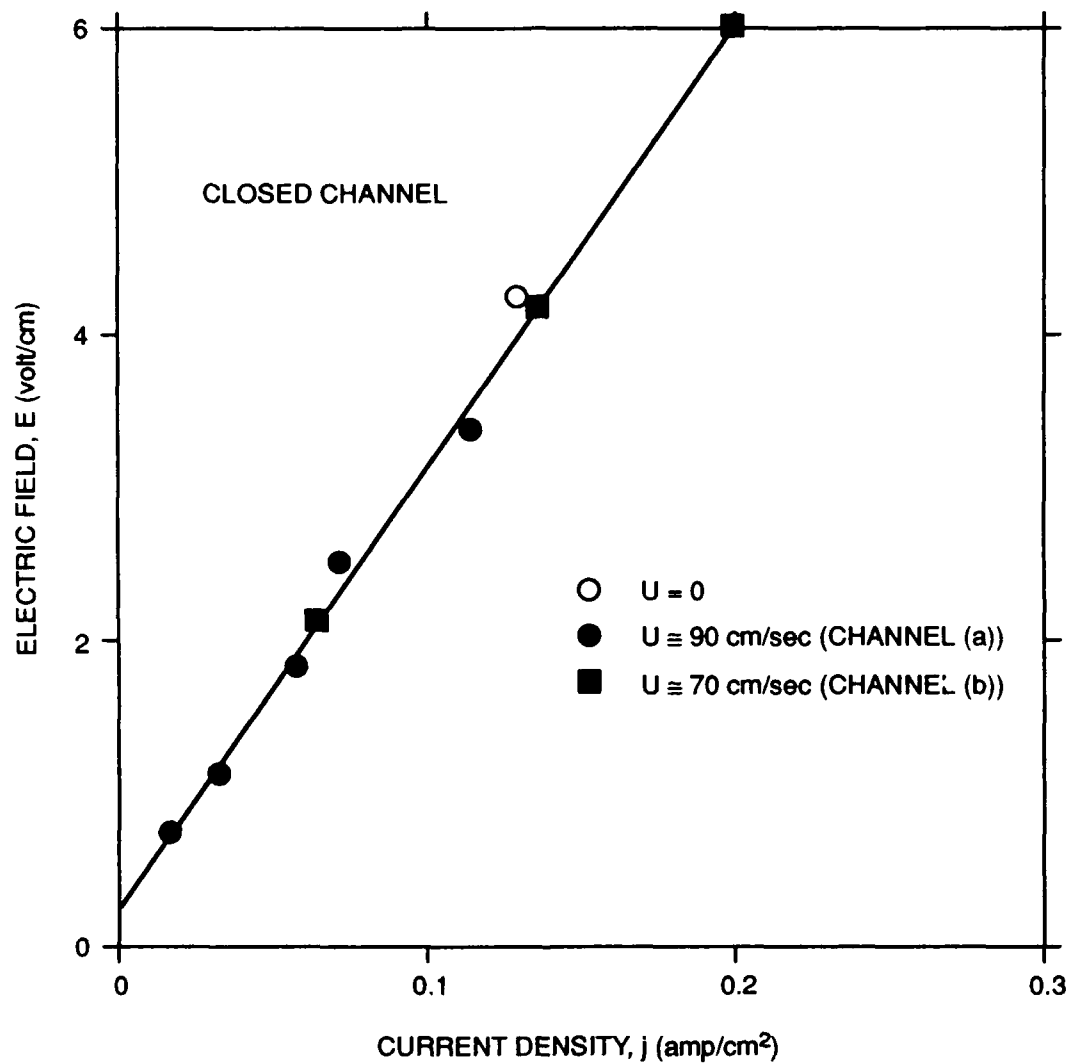
**Fig. 9.** Current density variation with electric field for an enclosed channel with aluminum electrodes.
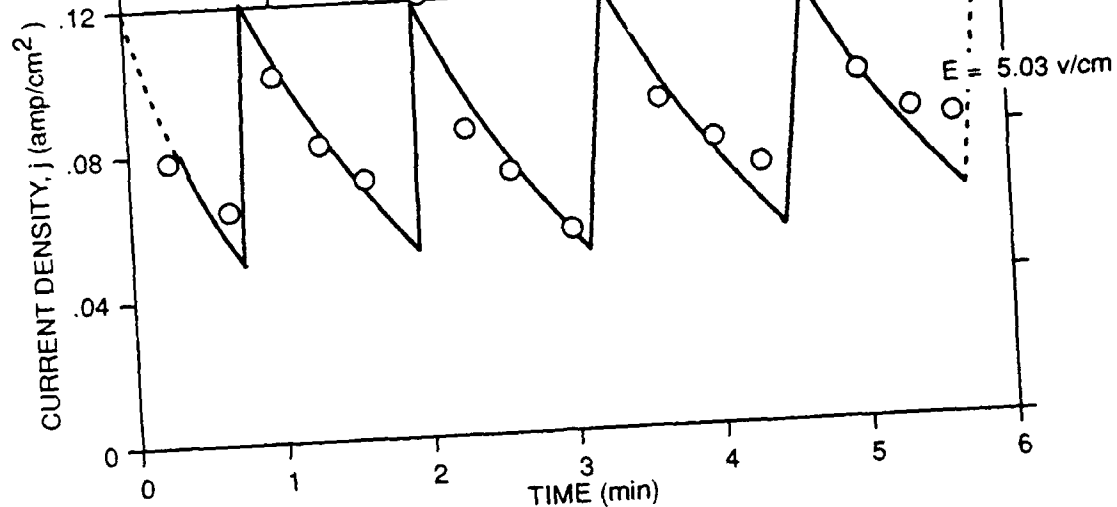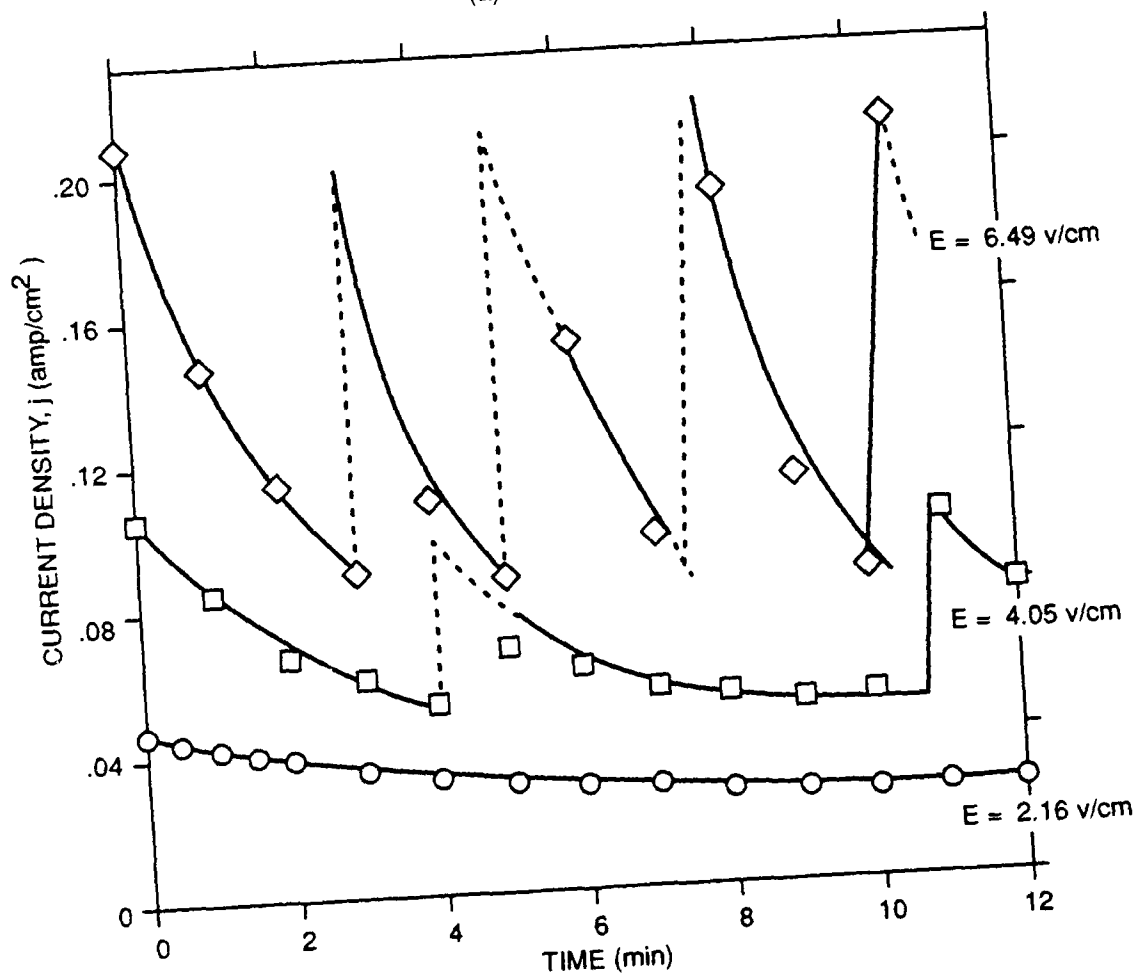
**Fig. 10.** Time variation of the current density in an enclosed channel with a horizontal top wall in the exit diffuser.
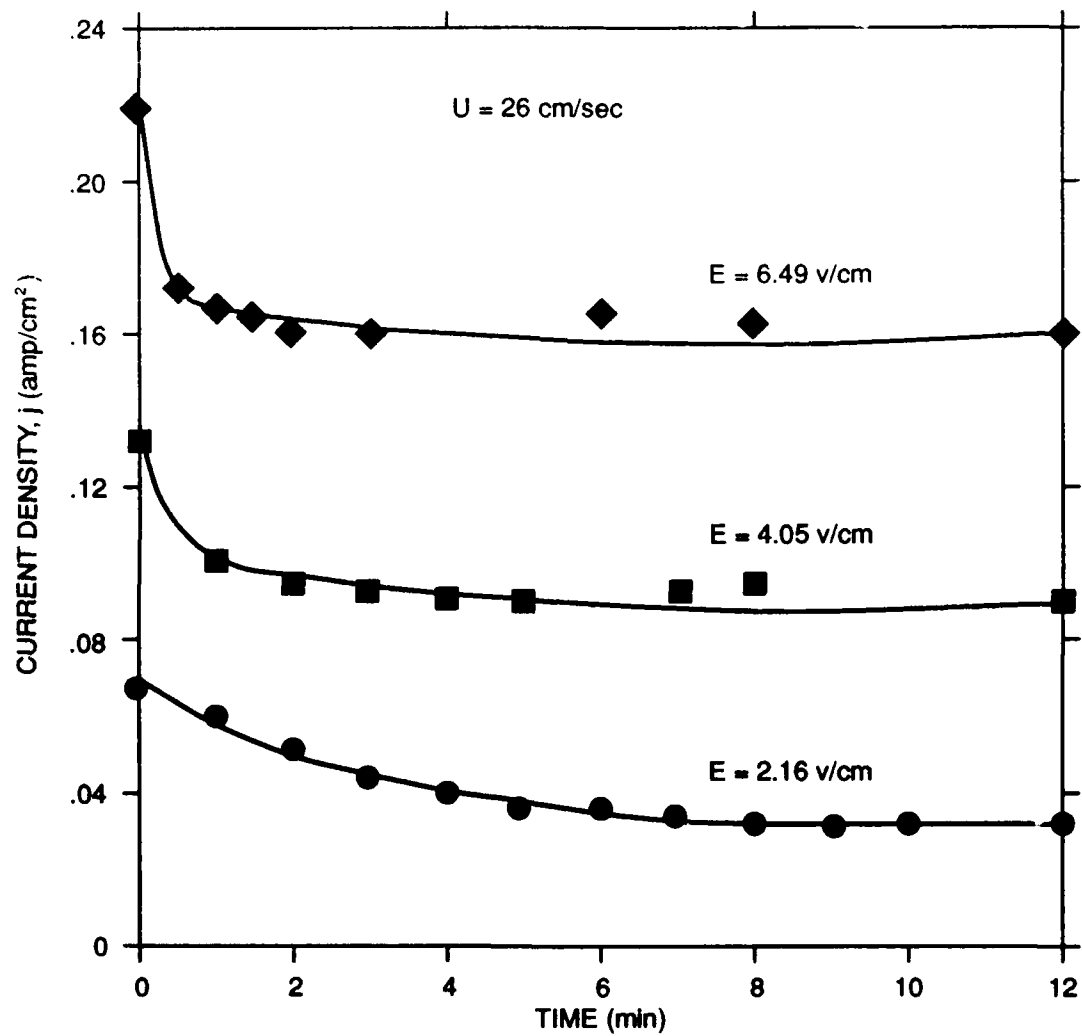
**Fig. 11.** Time variation of the current density in an enclosed channel with a 2° diverging top wall diffuser.
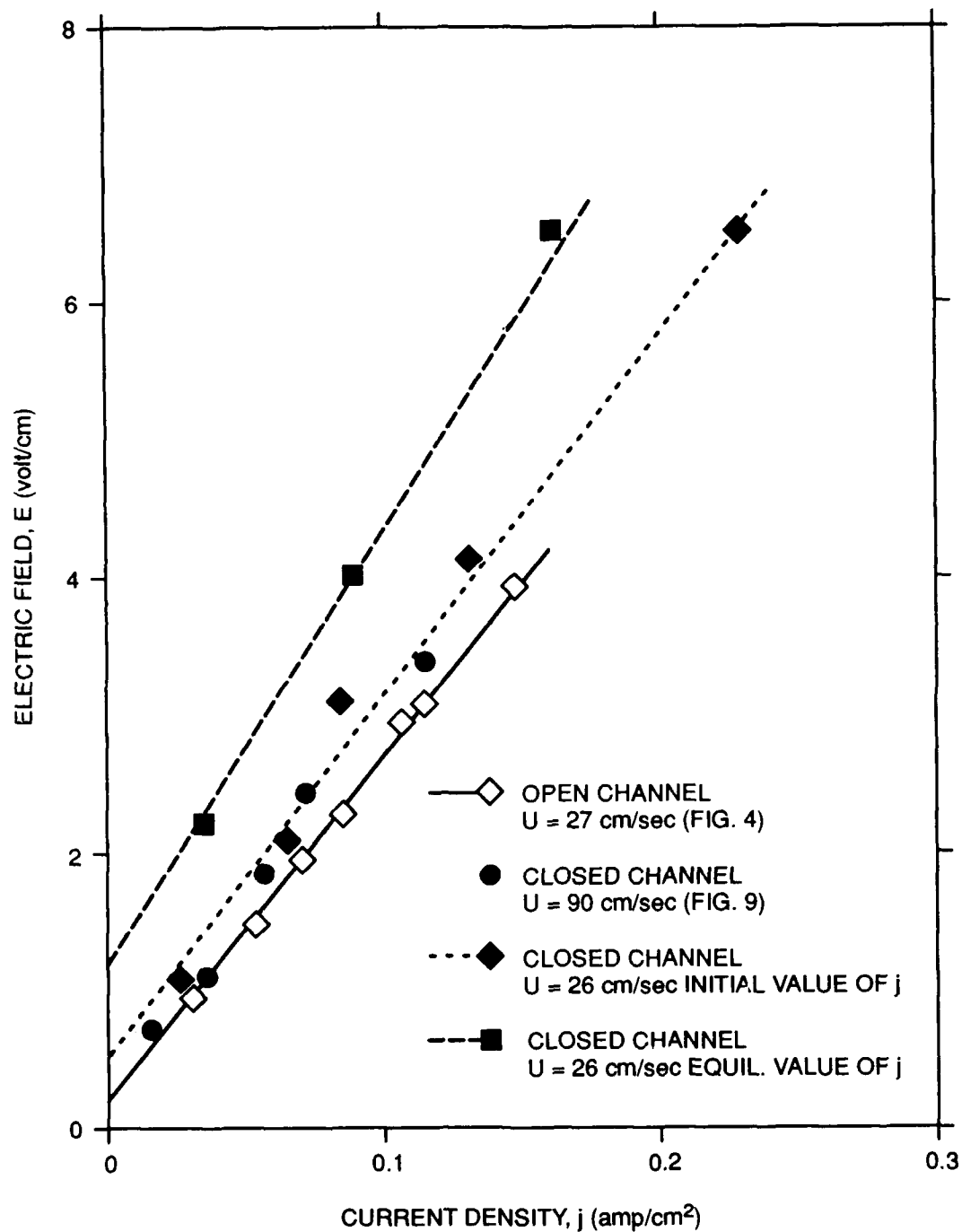
**Fig. 12.** Current density variation with electric field for an enclosed channel at various run conditions.

(a) Photo of surface foam on the cathode wall.



FOAM BOUNDARY LAYER
ON FREE SURFACE

FREE SURFACE

FLOW INTO THE PAGE

ANODE

CATHODE

FEWER
BUBBLES

NO BUBBLES
IN THE
FREE STREAM

BUBBLE ON WALL

FREE BUBBLES
RISE VERTICALLY

BOTTOM WALL (FLOOR)
BOUNDARY LAYER REGION –
NO BUBBLES
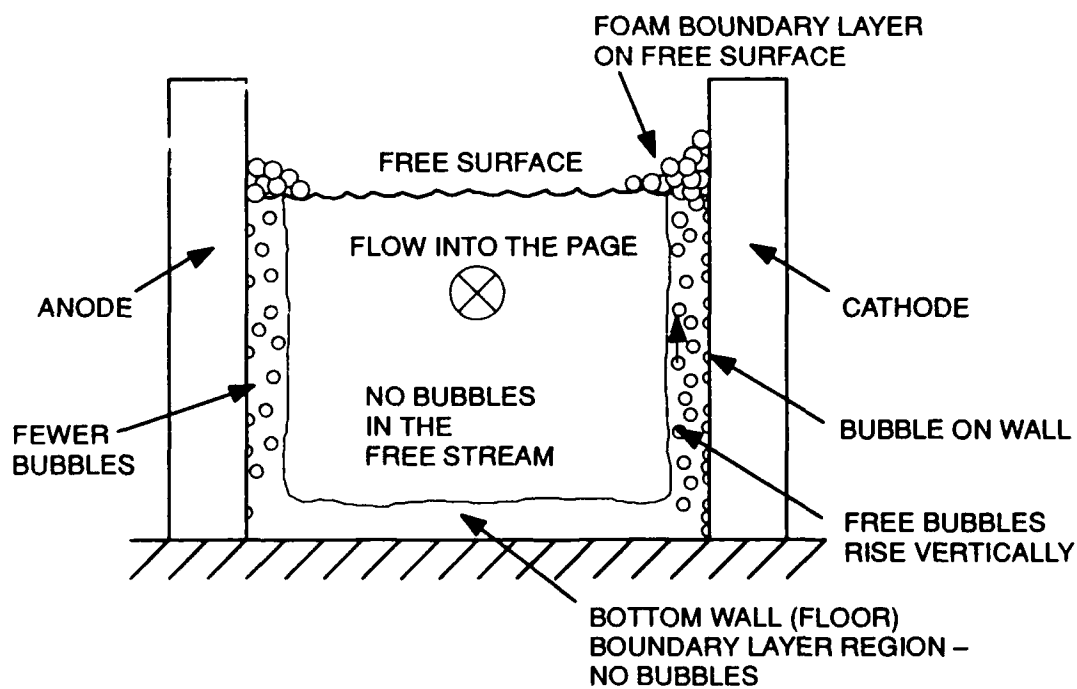
(b) Cross-sectional sketch of the bubble movement pattern.

**Fig. 13.** Hydrogen bubble dynamics in an open-top channel.
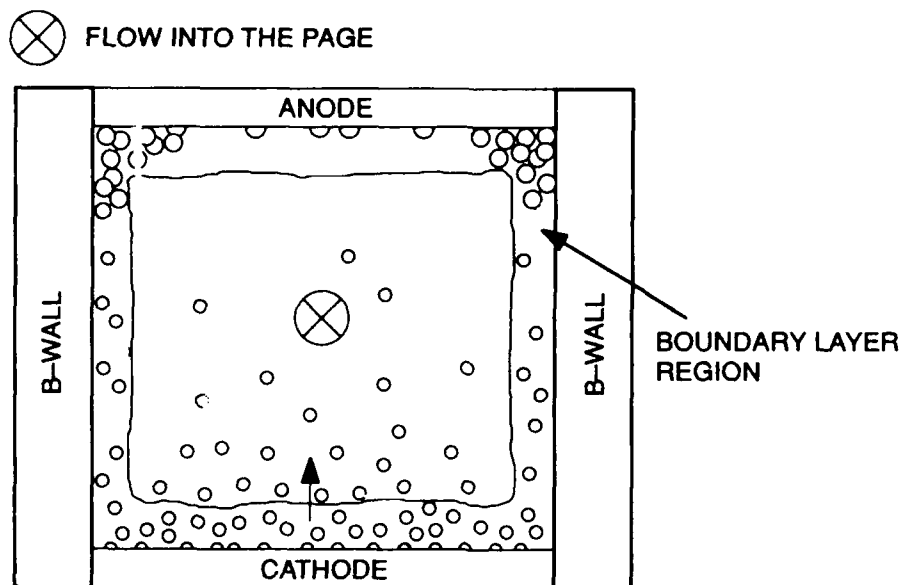
(a) Cathode floor and anode ceiling.
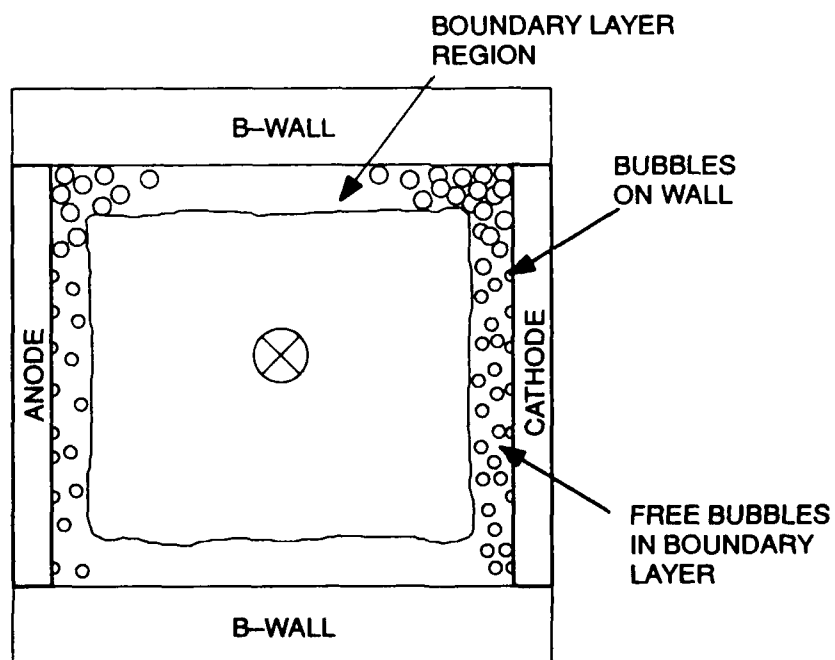
(b) Electrodes on the sidewalls.

**Fig. 14.** Hydrogen bubble dynamics in a closed channel with different electrode

INLET SUPPORT VANES    OUTER BODY ELECTRODE    EXIT VANES

FLOW ⟶    $\vec{u}$    $\vec{J}$
⊙ $\vec{B}$    ⟶    ↑    ⊙ $\vec{B}$

INNER BODY ELECTRODE

⊗ $\vec{B}$    ANNULAR FLOW PASSAGE    ⊗ $\vec{B}$

INLET & EXIT VANES SUPPORT THE INNER BODY
AND ENCLOSE THE MAGNET WINDINGS WHICH PRODUCE
AN AZIMUTHAL $B$-FIELD
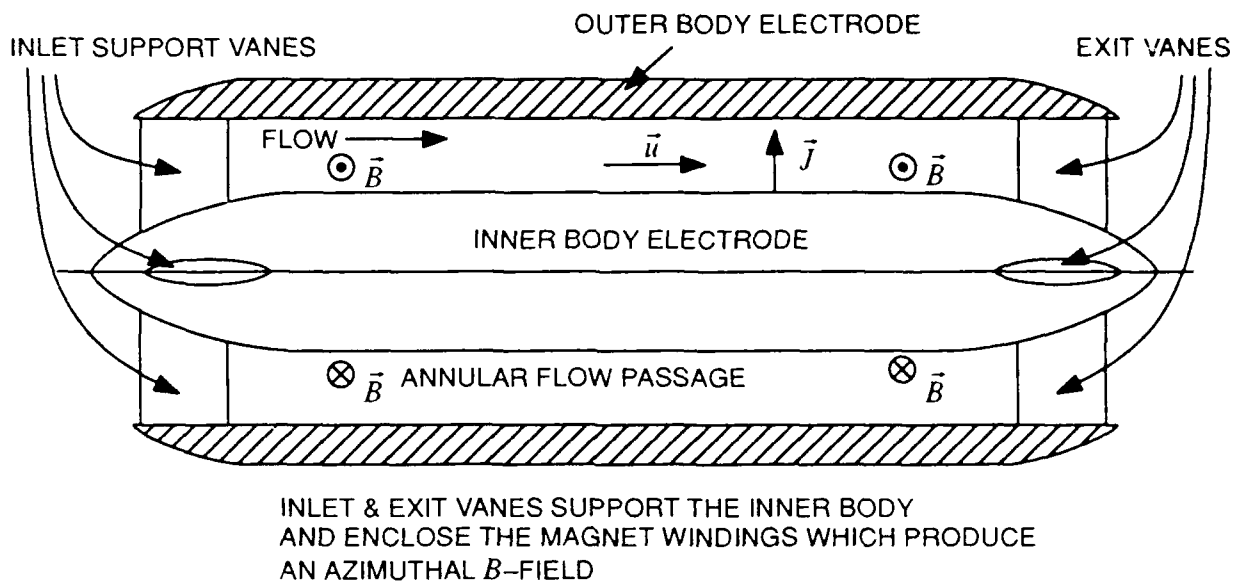
(a) Sketch of the toroid configuration.

BOUNDARY LAYER
REGIONS

$\vec{B}$

$\vec{j}$

CENTER
BODY

CATHODE-
WALL

ANODE
WALL

⊗    FLOW INTO THE PAGE
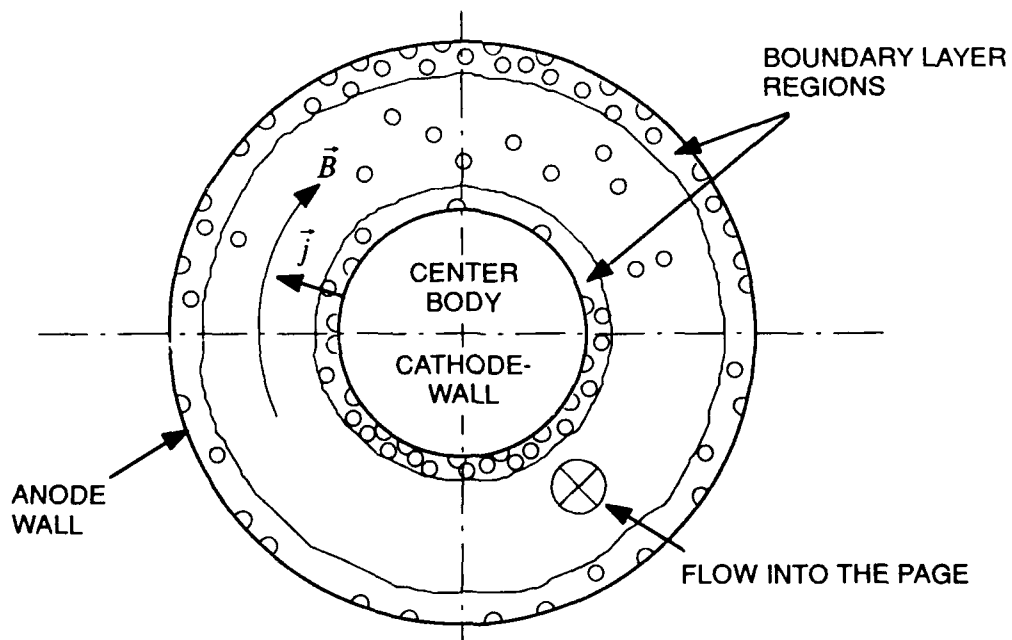
(b) Prospective bubble pattern with a toroid annulus thruster.

**Fig. 15.** Annular toroid configuration.
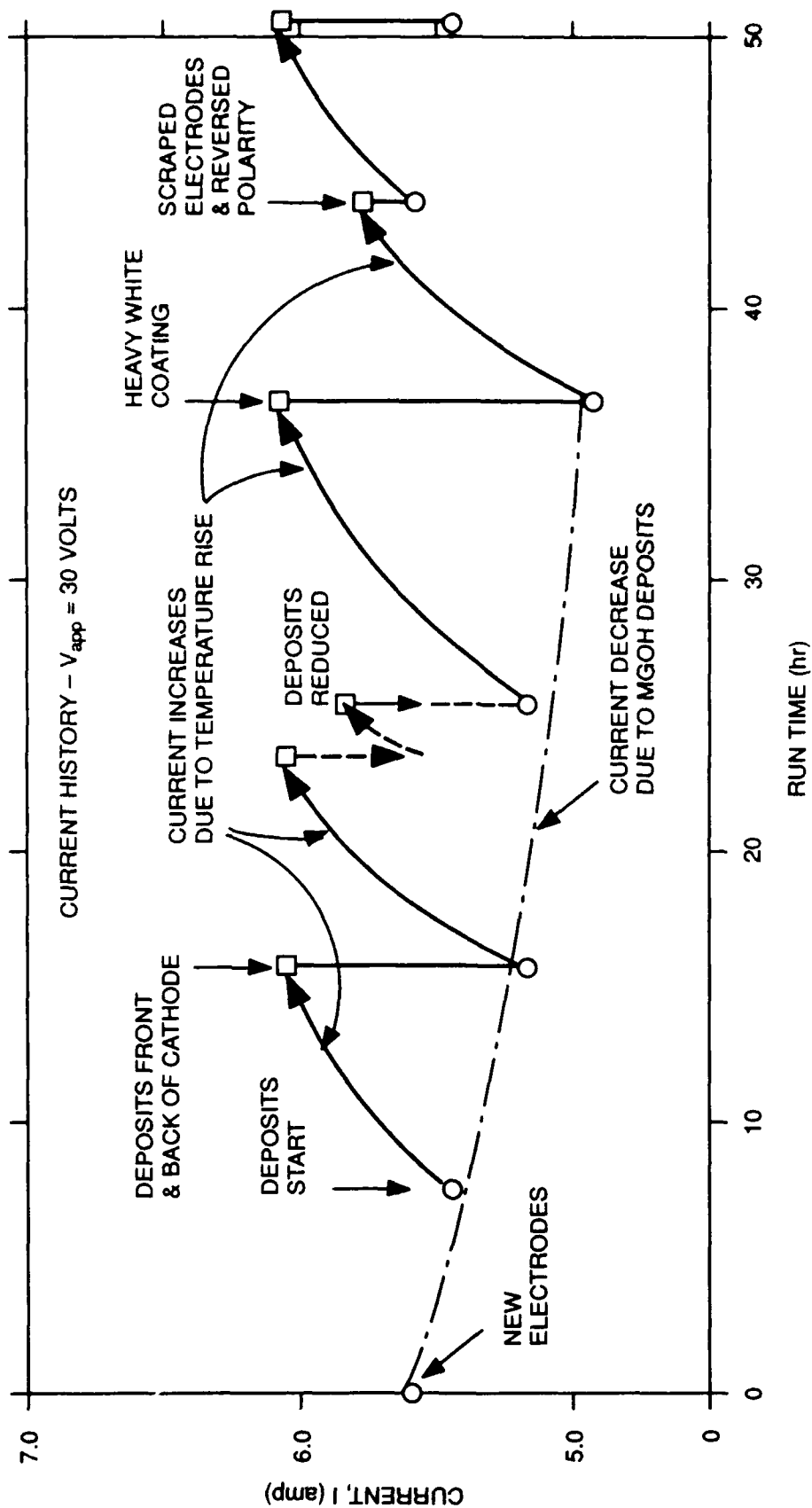
**Fig. 16.** Current history over a 50-hour test of Eltech anode and Eltech cathode.
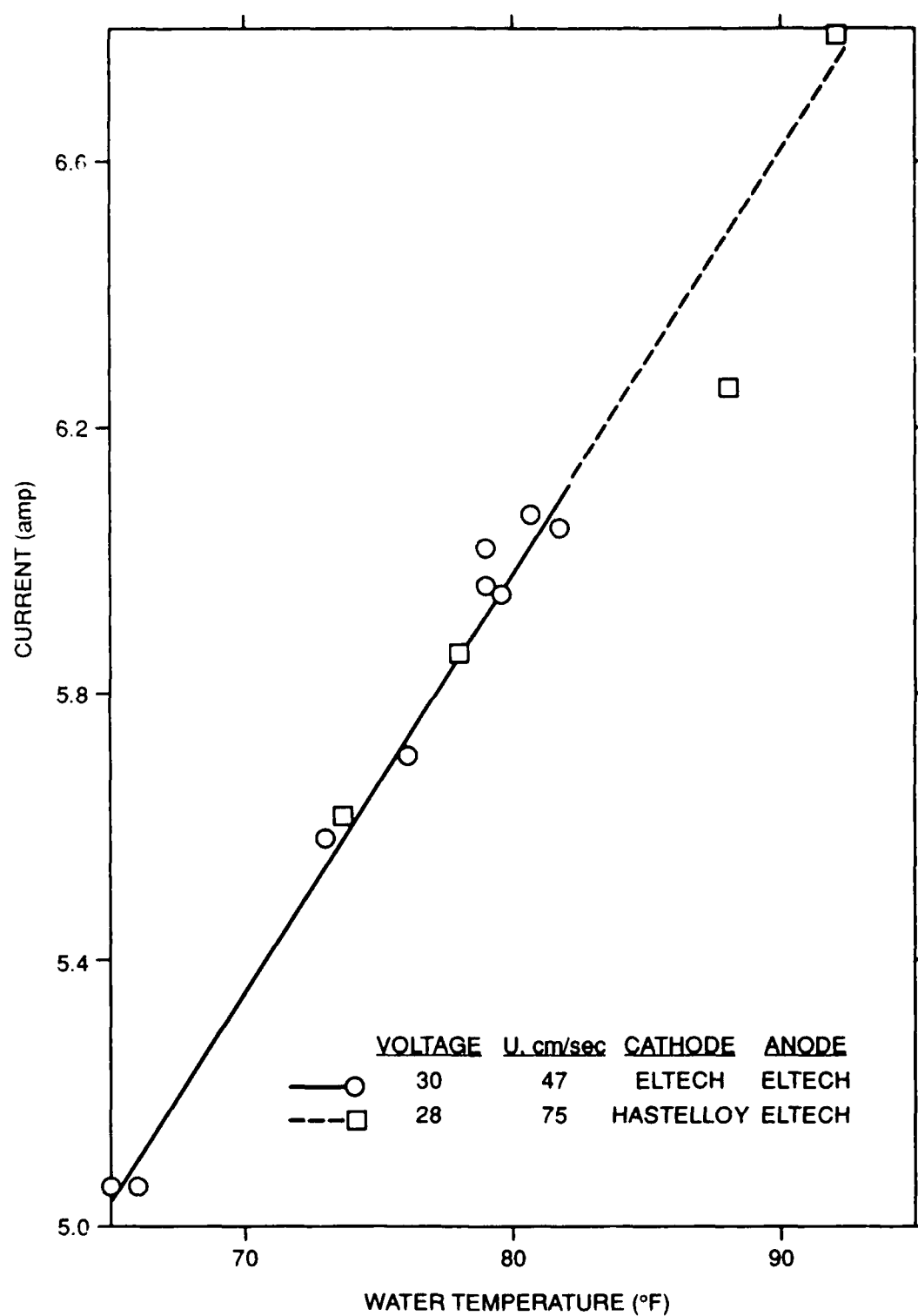
**Fig. 17.** Variation of electrode current with water temperature during long-duration tests.
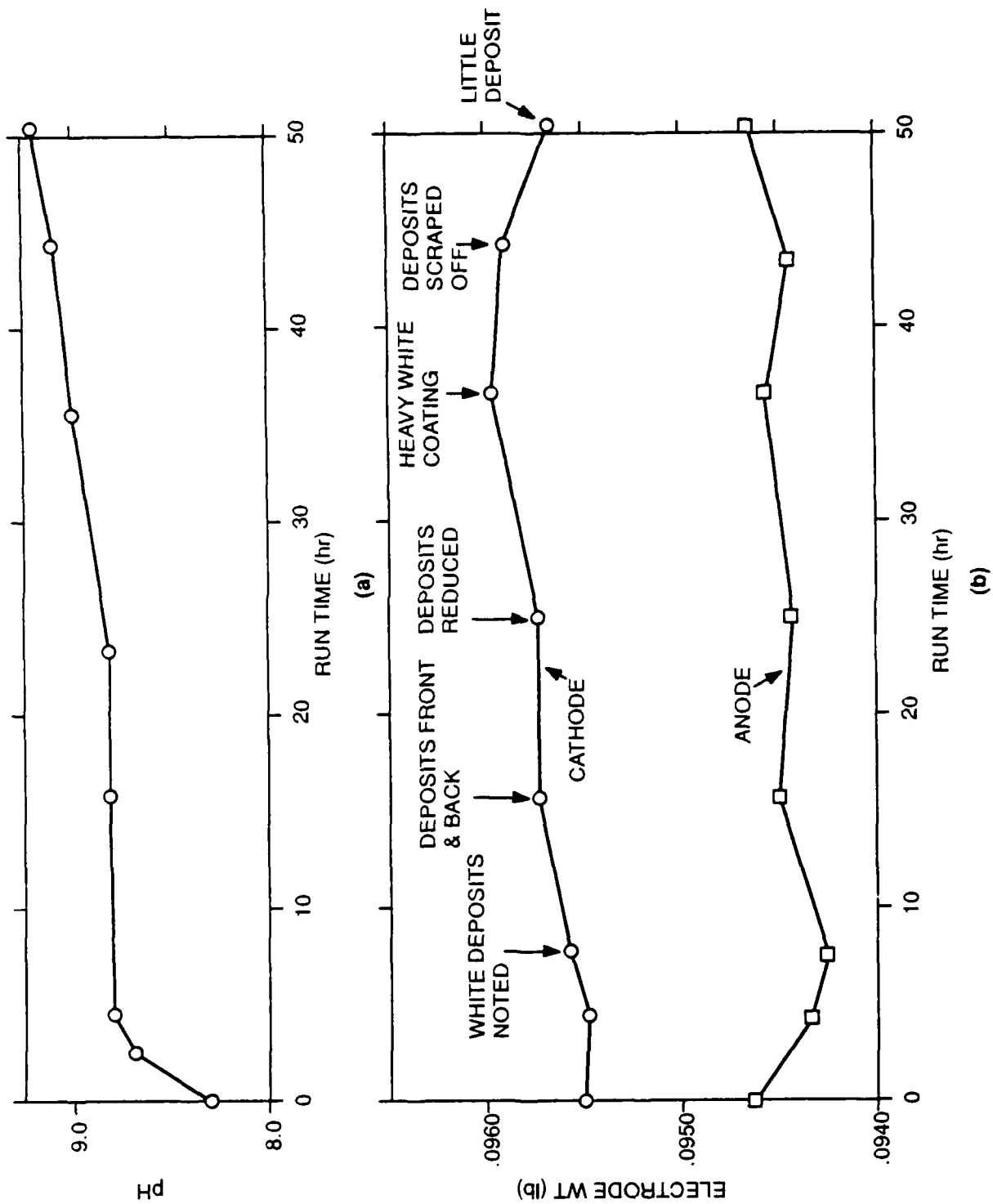
**Fig. 18.** Some results of long-duration testing.
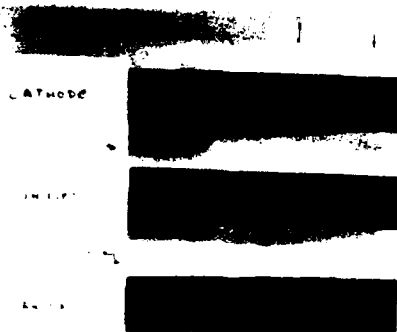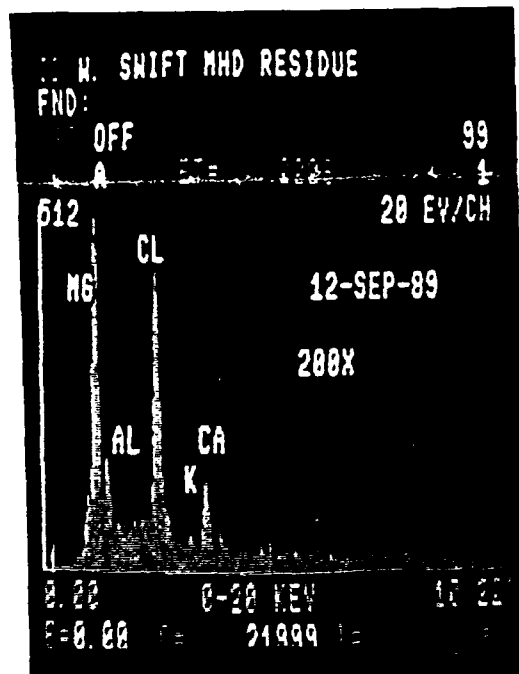
(a) After 15.5 hours of testing.
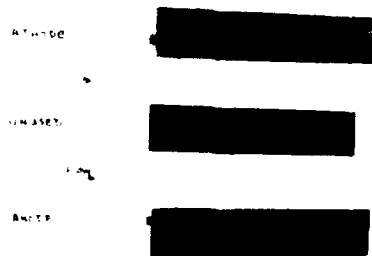


(b) After 36.3 hours of testing.

Fig. 19. Photos of Eltech DSA® electrodes during 50-hour test.

# APPENDIX A
## CHEMICAL ANALYSIS OF CATHODE DEPOSIT

| Bill Swift fs=1k 0.07 | 95357 9/13/89 | white material | |
|---|---|---|---|
| 2Theta | d | I | ID |
| 11.5 | 7.741 | 22vd | m(100) |
| 18.83 | 4.730 | 11d | h(90) |
| 20.5 | 4.347 | 10vvd | |
| 23 | 3.878 | 10vvd | m |
| 26.4 | 3.365 | 4 | ca(100) |
| 27.3 | 3.275 | 2 | ca |
| 29.5 | 3.035 | 21s | cc(100) |
| 33.15 | 2.708 | 5s | ca |
| 34.8 | 2.583 | 23d | m |
| 35.12 | 2.491 | 7s | ca |
| 38.1 | 2.366 | 45 | h(100) |
| 39.45 | 2.288 | 25d | m,cc |
| 40.6 | 2.226 | 3 | |
| 41.2 | 2.195 | 4 | ca |
| 43.2 | 2.097 | 5 | cc |
| 46 | 1.976 | 8d | ca |
| 46.45 | 1.958 | 3 | m |
| 47.1 | 1.932 | 6 | |
| 47.5 | 1.917 | 7 | cc |
| 48.25 | 1.889 | 6 | ca |
| 48.6 | 1.876 | 6 | cc |
| 50.25 | 1.818 | 8du | ca |
| 50.8 | 1.800 | 13vdu | h |
| 53.05 | 1.728 | 7s | ca |
| 58.75 | 1.573 | 25d | h |
| 60.1 | 1.541 | 14vdu | |
| 60.73 | 1.527 | 28d | m |
| 61.55 | 1.508 | 18ud | m |
| 62.05 | 1.497 | 27 | h |

h=Mg(OH)2 JCPDS 7-239
m=Mg6Al2(OH)18(4.5H2O) 35-965
cc=CaCO3 calcite 5-0543
ca=CaCO3 aragonite 5-0453

d=diffuse diffraction line
v= very; u=unresolved line
s=sharp line



W. SWIFT MHD RESIDUE
FND:
OFF 99
A 1
512 20 EV/CH
MG CL 12-SEP-89
200X
AL CA
K
0.00 0-20 KEV
F=0.00 21999

Comments
-----------------------------------------------------------
XRD-
Major: Mg(OH)2,
Mg6Al2(OH)18.(4.5H2O) type phase as per
JCPDS 35-965. note there are several
phases which have similar patterns to the above as
Mg6Al2CO3(OH)16(4H2O) JCPDS 14-191,and Al(OH)3
is possible.
An amorphous phase(s) also present
Minor: CaCO3 calcite and aragonite forms detected

note: Ca(OH)2, NaCl, CaCl2, MgCl2 not detected
The amorphous phase(s) maybe the chloride
containing component.

SEM-EDX-
Mg>Cl>>Ca,Al>K

# REFERENCES

1. Friauf, James B, "Electromagnetic Ship Propulsion" ASNE Journal, p. 139-142. (Feb 1961).

2. Phillips, Owen M., "The Prospects for Magnetohydrodynamic Ship Propulsion", Journal of Ship Research, p. 43-51 (Mar 1962).

3. Doragh, R.A., "Magnetohydrodynamic Ship Propulsion Using Superconducting Magnets", Presented Annual Meeting of The Society of Naval Architects and Marine Engineers, New York, NY. (14 & 15 Nov 1963).

4. Way, S., "Propulsion of Submarines by Lorentz Forces in the Surrounding Sea" ASME Publication 64-WA/ENER7, Winter Meeting (29 Nov - 4 Dec 1964).

5. Hummert, George T., "An Evaluation of Direct Current Electromagnetic Propulsion in Seawater" Office of Naval Research Report ONR-CR168-007-1 (Jul 1979).

6. Way, S., "Electromagnetic Propulsion for Cargo Submarines", Journal of Hydrodynamics, Vol. 2, No. 2 (Apr. 1968).

7. Tada, Eiichi, Y. Saji, K. Kuroishi, and T. Fujinaga, "Fundamental Design of a Superconducting EMT Ice Breaker", Trans. I Mar E (C), Vol 97, Conf. 3, Paper 6, p. 49-56.

8. Motora, S., S. Takezawa, and H. Tamma, "Research and Development of Superconducting Electromagnetic Propulsion Ships," Technical Report of Tsukuba Institute 9, (1), pages 1-9 (Apr 1989).

9. Motora, Seizo, S. Takezawa, and H. Tamama "Research and Development of Superconducting Electro-Magnetic Ships," paper presented at the 15th meeting of the U.S. Japan Cooperative Program in Natural Resources, Panel on Marine Facilities, Tokyo (9-10 May 1988).

10. Bennett, J.E., "Electrodes for Generation of Hydrogen and Oxygen from Seawater", Int. Journal of Hydrogen Energy, Vol 5, p. 401-408 (1980).

11. Bennett, John E., "On-Site Generation of Hypochloride Solutions by Electrolysis of Seawater, AIChE Symposium Series - Water (1977).

12. El-Bassuoui, A.M.A., J.W. Sheffield, and T.N. Veziroglu, "Hydrogen and Fresh Water Production from Seawater", Int. Journal of Hydrogen Energy, Vol 7, No. 12, p. 919-923 (1982).

13. Slipchenko, A.V., O.S. Saviuk, and Yu. S Bonsov, "Effect of Anion Composition of the Electrolyte on Active Chlorine Current Yield in the Electrolysis of Sea and Brackish Waters" Khiniya i Tekhnaloguya Vody (Translated to English) Vol. 9, No. 2 p. 150-152 (1987).

14. LeRoy, R.L. M.B.I. Janjua, R. Renaud, and U. Leuenberger,"Time-Variation in Unipolar Water Electrolysis and Their Implications for Efficiency Improvement", Proceedings of the Symposium on Industrial Water Electrolysis, Vol. 78-4, p. 63-76 (1978).

15. Richardson, E.G. (Ed), Technical Aspects of Sound, Chap. 5, "Air Bubbles in Water" by E. Meger, p. 222-238, Elsevier Publishing Co. (1957).

16. Rice, Warren A., U.S. Patent No. 2,997,013 (22 Aug 1961).

17. Resler, E.L., "Magnetohydrodynamic Propulsion of Sea Vehicles", Seventh Symposium on Naval Hydrodynamics, Rome Italy p. 1437-1445 (1968).

# INITIAL DISTRIBUTION

## Copies

3  DARPA/STP
LCDR Richard Martin
Advanced Technology
1515 Wilson Blvd., Suite 705
Arlington, VA 22209

3  ONT
Gene Remmers
Office of Chief of Naval Research
Office of Naval Techology
800 N. Quincy St.
Arlington, VA 22217–5000

12  DTIC

2  Dr. John S. Walker
University of Illinois at Urbana-
Champaign
Dept. Mech. & Ind. Engineering
144 Mechanical Engineering Bldg.
1206 West Green St.
Urbana, Illinois 61801

2  Dr. Daniel W. Swallom
Avco Research Laboratory
2385 Revere Beach Parkway
Everett, MA 02149

2  Dr. Michael Petrick
Argonne National Laboratory
9700 South Cass Ave.
Argonne, IL 60439

20  Dr. Kenneth E. Tempelmeyer
c/o Office of the Dean College of
Engineering and Technology
Southern Illinois University
Carbondale, Illinois 62901

2  Dr. Basil Picologlou
Engineering Physics Division
Argonne National Laboratory
9700 South Cass Ave.
Argonne, Illinois 60439

## CENTER DISTRIBUTION

| Copies | Code | Name |
|---|---|---|
| 3 | 01 | Richard E. Metry |
| 3 | 0113 | Dr. Bruce E. Douglas |
| 2 | 154 | Justin H. McCarthy |
| 2 | 1544 | Dr. Frank B. Peterson |
| 1 | 1561 | Geoffrey Cox |
| 1 | 1942 | Dr. Theodore M. Farabee |
| 2 | 27 | Larry J. Argiro |
| 2 | 2704 | Dr. Earl Quandt, Jr. |
| 2 | 271 | Howard O. Stevens, Jr. |
| 10 | 2711 | David E. Bagley |
| 2 | 2711 | Robert C. Smith |
| 10 | 2712 | Dr. Neal A. Sondergaard |
| 10 | 2712 | Dr. Samuel H. Brown |
| 2 | 2712 | Michael J. Supercznyski |
| 1 | 272 | Timothy J. Doyle |
| 1 | 2743 | David B. Larrabee |
| 1 | 3411 | Margaret L. Knox |
| 1 | 3421 | TIC Carderock |
| 2 | 3422 | TIC Annapolis |
| 10 | 3432 | Reports Control |